



Kent Academic Repository

Howard, Alexander Francis (2020) *Investigating the Role of Neuronal SKN-1 in C. elegans*. Master of Science by Research (MScRes) thesis, University of Kent,.

Downloaded from

<https://kar.kent.ac.uk/80065/> The University of Kent's Academic Repository KAR

The version of record is available from

This document version

Other

DOI for this version

Licence for this version

UNSPECIFIED

Additional information

Versions of research works

Versions of Record

If this version is the version of record, it is the same as the published version available on the publisher's web site. Cite as the published version.

Author Accepted Manuscripts

If this document is identified as the Author Accepted Manuscript it is the version after peer review but before type setting, copy editing or publisher branding. Cite as Surname, Initial. (Year) 'Title of article'. To be published in *Title of Journal*, Volume and issue numbers [peer-reviewed accepted version]. Available at: DOI or URL (Accessed: date).

Enquiries

If you have questions about this document contact ResearchSupport@kent.ac.uk. Please include the URL of the record in KAR. If you believe that your, or a third party's rights have been compromised through this document please see our [Take Down policy](https://www.kent.ac.uk/guides/kar-the-kent-academic-repository#policies) (available from <https://www.kent.ac.uk/guides/kar-the-kent-academic-repository#policies>).

Investigating the role of neuronal SKN-1 in *C. elegans*

A thesis submitted to the University of Kent for the degree of MRes
School of Biosciences

2019

Alexander Francis Howard

Declaration

No part of this thesis has been submitted in support of an application for any degree or other qualification of the University of Kent, or any other University or Institution of learning.

University of Kent
Master's by Research in Genetics
Investigating the role of neuronal SKN-1 in *C. elegans*
Alexander Francis Howard

Abstract

In *C. elegans*, the SKN-1/Nrf transcription factor is a crucial component for controlling responses to oxidative stress, redox balance, proteostasis, healthy ageing and improving lifespan. SKN-1 has three major isoforms that function independently of one another. SKN-1A and SKN-1C are localised in the *C. elegans* intestine and have been extensively studied. The third isoform, SKN-1B, is confined to two amphid chemosensory neurons in the head of *C. elegans* and is still relatively unexplored. Here, we investigate the role of SKN-1B in three major pathways that all contribute to longevity; the insulin/IGF-1 signalling (IIS) pathway, the endoplasmic reticulum unfolded protein response (UPR_{ER}) and mitochondrial morphology. Publications investigating the longevity effects of dietary restriction (DR) have also uncovered evidence that may suggest SKN-1B has a role here, and so therefore we also include conditional DR by two published methods; bacterial deprivation (BD) and liquid DR (IDR). We found that SKN-1B is not required for induction of DAF-16 nuclear localisation or expression upon DR, however nuclear localisation in SKN-1B mutant worms is short-lived compared to wildtype. Interestingly also, SKN-1B is required for increased expression of the DAF-16-target gene *sod-3* using the IDR protocol, but not in BD. It was also discovered that SKN-1B positively regulates *hsp-4* expression under non-stressed conditions, but it was not required for induction of *hsp-4* expression during ER stress caused by *ero-1* RNAi. In addition, the long-lived phenotype of *ero-1* RNAi does not require SKN-1B and therefore its only role may be in basal expression of UPR_{ER} components under normal conditions. Finally, we found that SKN-1B mutant worms exhibit a mitochondrial morphology defect characterised by an increased network fragmentation that resembles a starved phenotype. SKN-1B mutant worms have a normal N2 lifespan, and so this phenotype is of an unknown physiological consequence. This data together provides new insights into the role of the under-studied SKN-1B transcription factor which can hopefully offer new directions for investigation. It has been shown that SKN-1B has multiple complex roles in many signalling pathways through neuroendocrine modulation; this along with its emerging role in behaviour present an exciting new area of research.

Acknowledgements

First and foremost, I would like to thank Dr. Jennifer Tullet for giving me the opportunity to study a Master's by Research in her lab and for the never-ending support I have received from her.

Also, to all the lab members past and present: Dr Isabel Goncalves Silva, Dr. Max Thompson, Dan Scanlon and Nikolaos Tadaris-Pallas I want to thank you all too for your support, training and most importantly friendship to get through weekend-club.

I would also like to extend thanks to Dr. Ian Brown for the help and training he provided in TEM and sectioning of our worms.

Lastly, to my family that have gone above and beyond to keep spirits high and to keep me grounded.

Alexander F. Howard

Table of contents

Abstract.....	1
Acknowledgements.....	2
Table of contents.....	3
1 Introduction.....	4
1.1 SKN-1/Nrf transcription factors.....	4
1.1.1 SKN-1 isoforms, expression and function.....	4
1.1.2 <i>C. elegans</i> as a model organism.....	6
1.2 SKN-1 in <i>C. elegans</i> longevity pathways	7
1.2.1 Insulin/IGF-1 signalling.....	7
1.2.2 Dietary restriction and nutrient sensing.....	9
1.2.3 Endoplasmic reticulum unfolded protein response.....	11
1.2.4 Mitochondria and energy balance.....	13
1.4 Research aims.....	16
2 Materials and methods.....	17
2.1 Strains.....	17
2.2 List of reagents.....	17
2.3 Methods.....	18
2.4 Microscopy.....	21
2.5 Statistics.....	22
3 Results.....	23
3.1 <i>skn-1b::GFP</i> expression is increased by dietary restriction.....	23
3.2 DR-induced nuclear DAF-16 is short-lived in Δ <i>skn-1b</i> mutant worms.....	25
3.3 IDR, but not BD, demonstrates SKN-1B-dependent <i>sod-3::GFP</i> upregulation..	27
3.4 SKN-1B may be required for UPR _{ER} component expression but not induction.	29
3.5 SKN-1B is not required for the <i>ero-1</i> longevity phenotype.....	31
3.6 SKN-1B is important for mitochondrial morphology.....	33
4 Discussion.....	36
4.1 Generation of new <i>C. elegans</i> strains.....	36
4.2 SKN-1B and the IIS.....	36
4.2.1 Expression of <i>skn-1b::GFP</i> is BD and IDR responsive.....	36
4.2.2 DAF-16 localisation in response to DR is short-lived in Δ <i>skn-1b</i> mutants.	37
4.2.3 Expression of <i>sod-3::GFP</i> is SKN-1B dependent in IDR.....	38
4.3 SKN-1B and the UPR _{ER}	39
4.3.1 Expression, but not induction, of <i>hsp-4</i> is regulated by SKN-1B.....	39
4.3.2 <i>Ero-1</i> extends lifespan independently of SKN-1B.....	40
4.4 SKN-1B and the mitochondria.....	41
4.4.1 Δ <i>skn-1b</i> mutants have an associated mitochondrial morphology defect..	41
5 References.....	43
6 Supplementary information.....	48

Introduction

1.1 SKN-1/Nrf transcription factors

1.1.1 SKN-1 isoforms, expression and function

Skinhead-1 (SKN-1) is a *C. elegans* transcription factor, and the functional homologue of mammalian NF-E2-related factor (Nrf). SKN-1 and Nrf share conserved structures that includes a DIDLID motif for transcription initiation, Cap'n'Collar (CNC) domain and a basic region. Mammalian Nrf transcription factors also contain a basic leucine zipper (bZIP) domain required for dimerization and DNA binding (Figure 1A); therefore SKN-1 undergoes alternative DNA binding which involves association of the N-terminal DNA-binding domain to its cognate half-site, and recognition of an AT-rich sequence in the minor groove of SKN-1 binding regions.¹

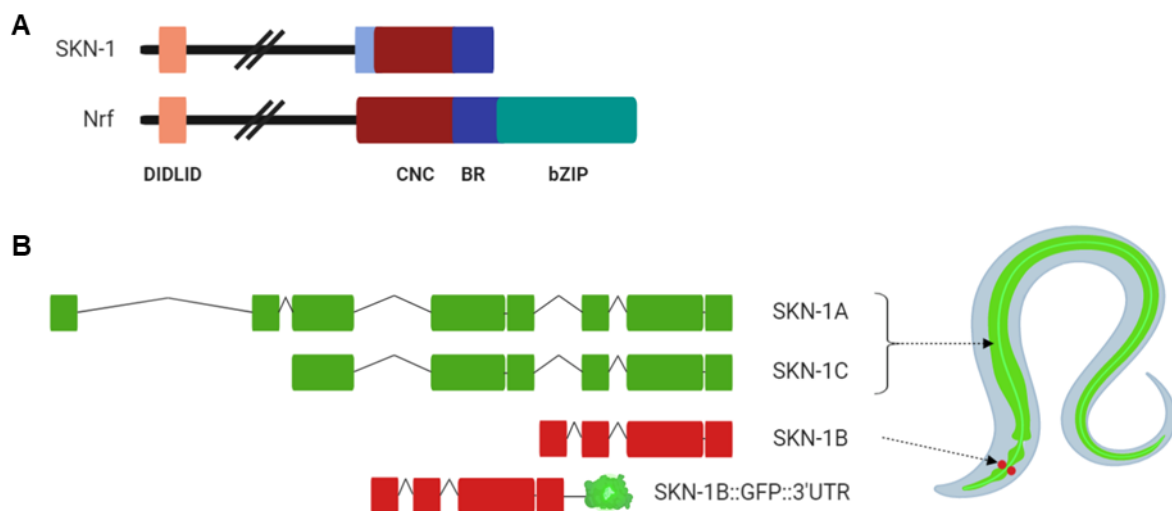


Figure 1 – SKN-1 structure and localisation

(A) Structure comparison between SKN-1 and the mammalian SKN-1 homologue Nrf. The SKN-1 DNA-binding region consists of CNC and BR motifs. (B) SKN-1A and SKN-1C are localised to the *C. elegans* intestine and are activated by independent mechanisms resembling Nrf-1 and Nrf-2 respectively. SKN-1B is confined to the ASI neurons of *C. elegans*. The *SKN-1B::GFP* model structure used in this paper is also shown. SKN-1D not shown. CNC; cap'n'collar, BR; basic region. Image created with BioRender. Adapted from Blackwell *et. al* 2015.

C. elegans expresses three major isoforms of SKN-1: SKN-1A, SKN-1B and SKN-1C. A fourth isoform, SKN-1D, is also predicted to occur naturally through alternative splicing but has not been confirmed *in vivo*. Only SKN-1A contains a transmembrane domain, and its mode of activation involves proteolytic cleavage of this domain for cytosolic release from the endoplasmic reticulum membrane; which most closely resembles the mammalian Nrf-1 isoform.² All other SKN-1 isoforms resemble the mode of action of the Nrf-2 transcription factor in mammals, which plays a role in the phase-II detoxification response that promotes cell survival through upregulation of genes controlled by antioxidant response elements (AREs). The Phase-II detoxification response is also upregulated in dietary restriction (DR) protocols, which contributes to the beneficial lifespan effect through Nrf-2 signalling pathways in rats.³

Expression of *skn-1* in the intestine of *C. elegans* is primarily composed of SKN-1A and SKN-1C isoforms (Figure 1B); however due to the N-terminal transmembrane domain of SKN-1A, this isoform seems to be confined to the ER and mitochondrial membranes prior to proteolytic cleavage. SKN-1C localisation shifts from cytoplasmic to nuclear in response to stress signals such as oxidative stress by paraquat, as well as impaired IIS signalling, to regulate genes involved in stress resistance and lifespan.^{4,5} Interestingly, SKN-1 activity in the intestine has also been shown to be dependent on the p38 mitogen-activated protein kinase (MAPK) pathway. Removal of p38/PMK-1 in *C. elegans* results in defective nuclear translocation of SKN-1 and greatly reduces the capacity of worms to respond to oxidative stressors such as sodium arsenite or paraquat.⁶

The complete function of SKN-1B is still relatively unknown, however this isoform is confined to neuronal cells. The *C. elegans* adult nervous system consists of 302 neurons, of which SKN-1B is expressed in the nuclei of two amphid chemosensory ASI neurons (Figure 1B).⁷ In experimental models of stroke, Parkinson's disease and Huntington's disease, Nrf-2 activation has a neuroprotective effect by delaying neuronal degeneration,^{8,9,10} though this has not been shown to be a mechanism of neuronal SKN-1B. Very little is known about the SKN-1B isoform in *C. elegans*, however this particular isoform has many suggested roles as a key component

of foraging and behavioural processes, as well as sensory integration, tissue coordination and has been previously shown to be required for one dietary restriction protocol to extend lifespan.⁷

1.1.2 *C. elegans* as a model organism

The use of *Caenorhabditis elegans* as a model organism to study ageing and age-related disease is still a relatively new and constantly evolving field; though it was in 1963 that Sydney Brenner proposed the use of *C. elegans* to investigate developmental biology and the CNS in higher eukaryotes. Today, studies involving *C. elegans* have made a large impact in many branches of research including development, evolution, age-related health and most notably diseases of ageing.

C. elegans is a free-living primarily hermaphroditic nematode, with males developing as a result of nondisjunction in the hermaphroditic germ line inducible by stress.¹¹ The adult worm consists entirely of 959 somatic cells that have had their function and lineage determined^{12,13,14}; in addition, *C. elegans* was the first multicellular organism to have its full genome sequenced, making them ideal for genetic studies.¹⁵ Hermaphrodite worms can lay up to 300 eggs during their lifetime and those fertilised by a male can lay up to 1000; in this way, induction of male worms and genetic crosses are very easily achievable as single worms can be selected to produce clonal populations before genotyping.¹¹

The time for development of an egg to an adult worm is around 72 hours at 25°C, with lifespan of wildtype (N2) worms averaging at around 20 days; making it an ideal model for ageing studies. In addition, the body of *C. elegans* is entirely transparent which makes it possible to easily image fluorescently tagged protein in live worms. The proteome of *C. elegans* has been reported to share 83% homology to humans¹⁶ and can be readily manipulated by a process known as RNA interference (RNAi), which involves simply incorporating dsDNA-expressing bacteria into their food source to silence specific protein coding mRNA.¹⁷

1.2 SKN-1 in *C. elegans* longevity pathways

1.2.1 Insulin/IGF-1 signalling

The insulin/IGF-1 signalling (IIS) pathway in *C. elegans* is a divergent pathway that transposes nutrient signals, in the form of insulin-like peptides (ILPs), to transcriptional programs that can alter the organisms' metabolic rate, development, behaviour and lifespan. Activation of the DAF-2/IGFR receptor by ILPs in-turn switches on the AGE-1 phosphoinositide 3-kinase (PI3K), which initiates a kinase cascade resulting in the phosphorylation and cytoplasmic sequestration of the effector DAF-16/FoxO and SKN-1/Nrf transcription factors.¹⁸ Consequently, when the IIS pathway is inactive DAF-16/FoxO and SKN-1/Nrf freely enter the nucleus to regulate transcriptional programs involving stress resistance, redox balance, mitochondrial function, lipid metabolism and the unfolded protein response (UPR) (Figure 2). In the ASI neurons, SKN-1B is constitutively active and may be under the control of other associated factors, however in intestinal cells SKN-1A/C is cytosolic under low stress after being phosphorylated by GSK-3.¹⁹ Under stress, intestinal SKN-1A/C then accumulates in the nucleus and becomes transcriptionally active, which is dependent on the p38 MAPK.⁶

The *C. elegans* genome encodes only one insulin/IGF-1 receptor (IGFR) but is predicted to encode a much larger number of insulin-like peptides (ILPs), many of which still have incompletely known function. Genetic studies using knockout strategies have identified functions for most of the 40 known ILPs expressed by *C. elegans*, which includes roles in development, metabolism and age-related diseases with some functional redundancy between ILP members.²⁰ It is also important to note that most ILPs are expressed in neuronal tissue, although there has been evidence of ILP regulation in other tissues including the intestine.²¹

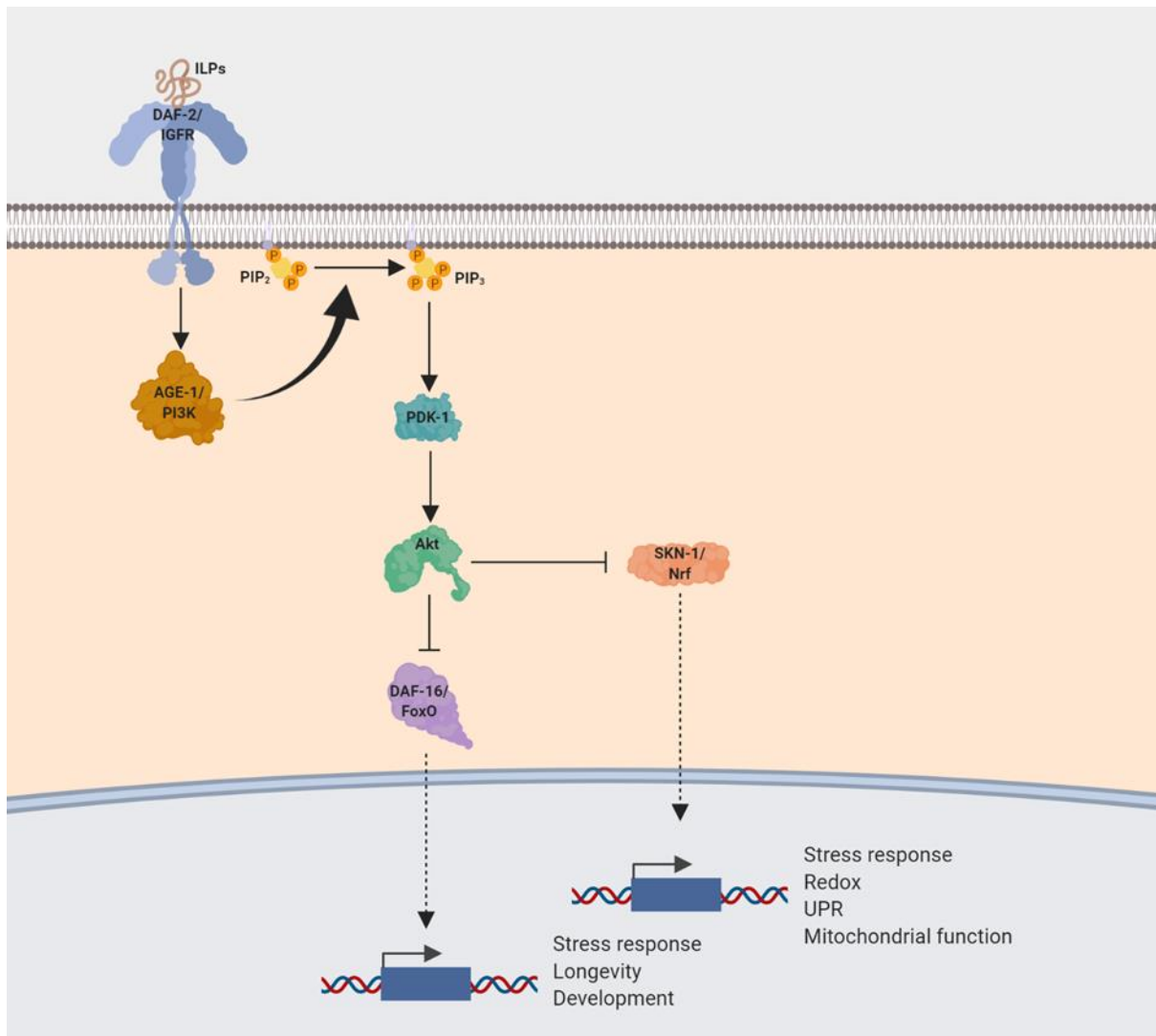


Figure 2 – Insulin/IGF-1 signalling (IIS) pathway in *C. elegans*

In *C. elegans*, the IIS pathway is initiated by small insulin-like peptides (ILP) that cause DAF-2/IGFR receptor dimerisation and signalling through a conserved phosphorylation cascade homologous to mammalian PI3K signalling. The culmination of this pathway is the phosphorylation and inactivation of DAF-16/FoxO and SKN-1/Nrf. Active DAF-16/FoxO and SKN-1/Nrf in the absence of IIS signalling regulate genes involved in (oxidative) stress responses, development, UPR, mitochondrial function and therefore longevity. Created with BioRender. Signalling information obtained from KEGG.

The importance of the IIS in the context of ageing came when it was discovered that genetic mutations of the *daf-2* and *age-1* genes significantly increased the lifespan of worms, as well as giving a protective resistance to many forms of stress.²² The effect of increased lifespan after inhibition of IIS is dependent on SKN-1 and DAF-16 transcription factors, which translocate to the nucleus of intestinal cells to mount a phase-2 detoxification response.⁵ In addition, transgenic expression of SKN-1 rescues the effects of impaired IIS signalling;

suggesting that the observed effects are primarily dependent on SKN-1, specifically intestinal SKN-1C.⁵

Genetic ablation of IIS signalling components in the ASI neurons, such as DAF-2/IGFR, reduces the capacity for chemosensation and results in a DAF-16-dependent extension to lifespan, also influencing the expression of downstream ILPs.^{23,24} In addition, SKN-1B expression in the ASI neurons is a requirement for some DR protocols to extend lifespan, however overexpression of SKN-1B alone is not sufficient to increase lifespan.⁷ The control of ILP expression is central to the coordination of distal tissues to the external cues detected by sensory neurons; as these ILPs are transported by vesicles to other tissues in order to arouse a second IIS activation in different cell types, this is sometimes referred to as ILP-to-ILP signalling.^{25,26} This mechanism is poorly characterised, however ASI-specific SKN-1B probably has an integral role in the regulation of tissue coordination and has been shown to affect the expression of some ILPs such as *ins-7* in the intestine (unpublished). In addition, the ASI neurons have been further implicated in regulating lifespan dependent of DAF-7/TGF- β .²⁷ The DAF-7/TGF- β pathway has also been shown to interact with IIS in manner that is still not fully understood, and it is not known whether ASI-specific SKN-1B and DAF-7/TGF- β have any cooperative effect on regulating lifespan.

1.2.2 Dietary restriction and nutrient sensing

Dietary restriction (DR) in *C. elegans* is a method of reducing food intake without causing malnutrition and is well known to extend lifespan as well as delay age-related disease.²⁸ DR may include specific methods such as caloric restriction, involving the omission of particular components in the diet, or intermittent fasting. There are many methods of DR that have been developed by independent laboratories, including genetic mutants, deprivation of food, dilution of food or axenic culture media; which is summarised in table 1.

Table 1 – Methods of dietary restriction

Various methods of dietary restriction that have independent longevity affects; lifespan extension is relative to the age of worms when DR began (birth, larval or adult). CDLM; chemically defined liquid medium, DP; dilution of peptide, DD; dietary deprivation, bDR; bacterial dietary restriction, BD; bacterial deprivation, sDR; solid dietary restriction, IDR; liquid dietary restriction.

Method	Medium	Food Source	Mutation	Lifespan Extension	Reference
Control	Solid	Live <i>E. coli</i>	/	/	/
<i>eat-2</i>	Solid	Live <i>E. coli</i>	<i>eat-2</i>	≤ 57%	[29]
Axenic	Liquid	Chemical broth	None	≤ 150%	[30]
Resveratrol	Solid	<i>E. coli</i>	None	≤ 14%	[31]
CDLM	Liquid	Chemical broth	None	≤ 88%	[32]
DP	Solid	Live <i>E. coli</i>	None	≤ 33%	[33]
DD	Solid	No <i>E. coli</i>	None	≤ 50%	[34]
bDR	Liquid	Live <i>E. coli</i> +AB	None	≤ 73%	[35]
BD	Solid	No <i>E. coli</i>	None	≤ 29%	[27]
sDR	Solid	<i>E. coli</i>	None	≤ 35%	[36]
IDR	Solid + Liquid	Live <i>E. coli</i> +AB	None	≤ 28%	[7]

Of these methods, those used in this study include IDR and BD. The IDR method involves both a liquid and solid phase, where worms are placed into suspension of bacteria at a pre-defined concentration in series. In one study using this method, bacterial dilution was found to extend lifespan up to ~28% at an intermediate dilution (2.5×10^7 CFU/mL) but interestingly found that further dilution and complete bacterial deprivation were not beneficial and actually detrimental to lifespan respectively.⁷ This effect is protocol-specific, as other labs have demonstrated an extension to lifespan during complete bacterial deprivation,³⁴ and this discrepancy may be caused by behavioural changes associated with the sensory perception of liquid vs. solid media.³⁷ These behavioural changes could directly interfere with the feeding ability of the worms, or may be indicative of changes to IIS signalling intermediates DAF-2 or

DAF-16 which are linked to swimming and quiescent behaviours³⁷ though this is unclear. The IDR method however has been shown to extend lifespan in a manner that is dependent on SKN-1B, as overexpression of SKN-1B in the ASI neurons rescued the longevity defects displayed by *skn-1(zu135)* worms (genetic null mutation affecting all SKN-1 isoforms);⁷ thus making it an essential method in exploring the role of SKN-1B in the context of DR. The BD method more simply involves transferring worms to culture plates without any food source. This method also can extend lifespan to a similar level as IDR and also requires ASI-specific factor DAF-7/TGF- β for this phenotype.²⁷ DAF-7/TGF- β is intimately linked with IIS signalling and involves cross-regulation that is poorly defined, and could possibly implicate neuronal SKN-1B.

1.2.3 Endoplasmic reticulum unfolded protein response

The endoplasmic reticulum unfolded protein response (UPR_{ER}) is a protective pathway that acts as a failsafe for cells undergoing proteostatic stress with either defensive or apoptotic outcomes. Before the UPR_{ER} is involved, the ER utilises a quality control mechanism called the ER-associated degradation (ERAD) pathway; in which unfolded proteins are targeted for degradation by the proteasome after export from the ER lumen (Figure 3B).³⁸ An overloading of the ERAD pathway during significant cellular stress will then trigger one of three parallel UPR_{ER} pathways regulated by ER transmembrane proteins (Figure 3C). The IRE-1 pathway begins with the release of inhibitory HSP-4/BiP due to accumulation of misfolded protein, resulting in receptor dimerisation.³⁹ IRE-1 dimers with active endoribonuclease functions can then cleave XBP-1 mRNA for translation of spliced XBP-1; the XBP-1 transcription factor regulates genes including ER chaperone proteins, folding enzymes, ERAD factors and ER stress recovery.⁴⁰ The PERK pathway similarly begins with dissociation of HSP-4/BiP and dimerisation; active PERK can then phosphorylate the eIF2 α translational initiation factor to reduce global translation in order to reduce ER workload. Active eIF2 α can also activate the ATF-4 transcription factor which switches on genes involved in redox homeostasis and the pro-apoptotic transcription factor CHOP.⁴¹ Finally, the ATF-6 pathway is initiated by

accumulation of misfolded protein in the ER lumen and translocation of the ATF-6 protein to the golgi body, where S1P/S2P proteases cleave ATF-6 into an active transcription factor. Genes regulated by ATF-6 include a myriad of protein chaperones, ERAD components and folding enzymes.⁴²

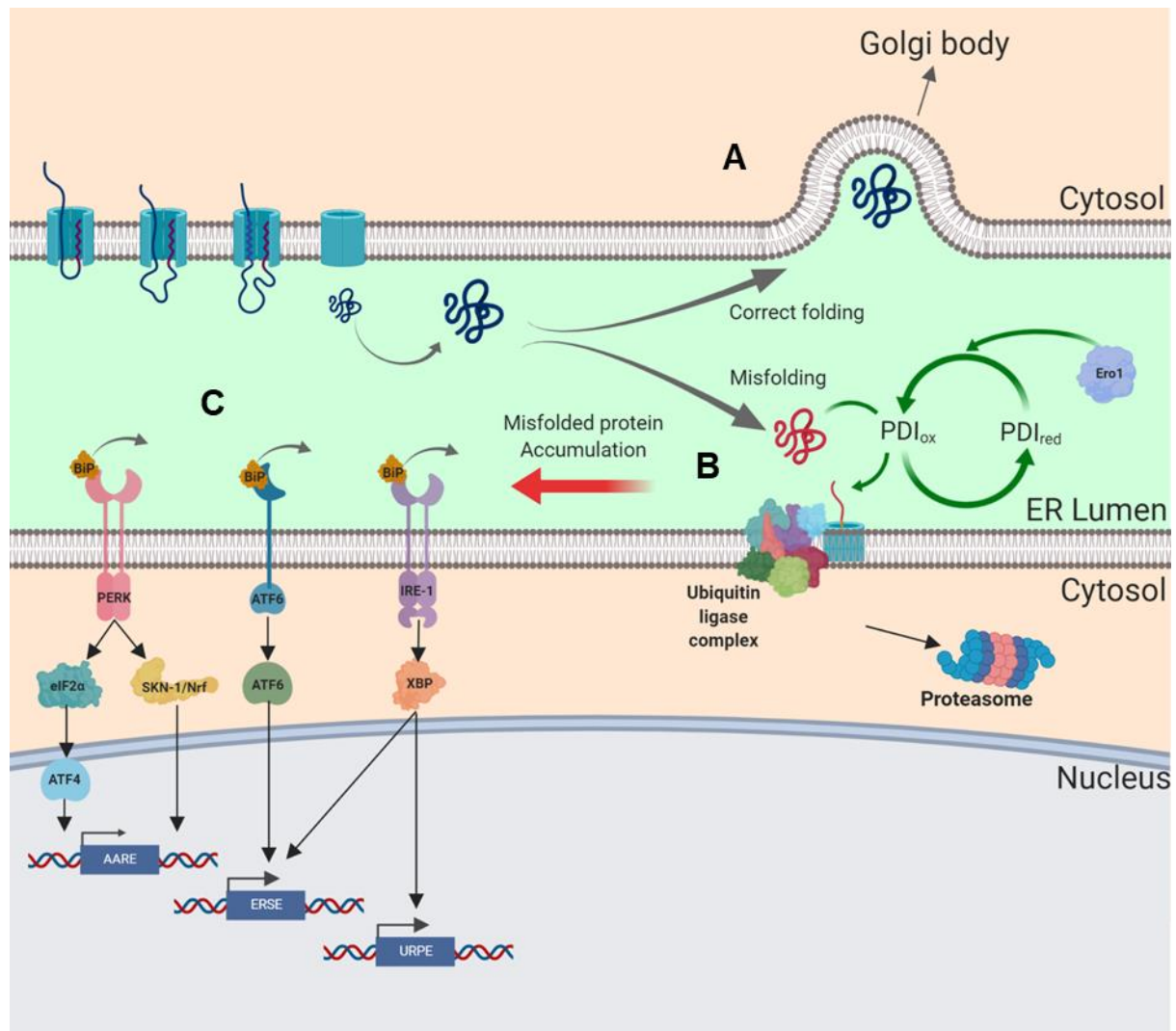


Figure 3 – The endoplasmic reticulum unfolded protein response (UPR_{ER}) in *C. elegans*

(A) Correct protein folding post-translation in the ER results in appropriate export and post-translational modification in the Golgi body. (B) The ER-associated degradation pathway (ERAD). PDI-1 promotes degradation by removing non-native disulphide bonds on misfolded protein; PDI-1 oxidation state is regulated by Ero-1. Following translocation and ubiquitin ligation, misfolded proteins are targeted to the proteasome for degradation. (C) Accumulation of misfolded protein during considerable stress results in activation of three signalling branches. AARE; amino acid response element, regulated by ATF-4 and SKN-1/Nrf for gene expression in amino acid metabolism, redox balance and ER stress recovery. ERSE; ER stress response element, regulated by ATF-6 and XBP-1 for genes involved in ER chaperone expression and ER stress recovery. URPE; unfolded response pathway element, regulated by XBP-1 for expression of ERAD factors. Created using BioRender. Signalling information obtained from KEGG.

SKN-1/Nrf has had an emerging role in the process of proteostasis, which is the cellular regulation of synthesis, folding, modification, trafficking and degradation of proteins. SKN-1/Nrf transcriptionally regulates many of the subunit genes for the proteasome and can compensate for a loss of function of the proteasome during cellular stress or during pharmacological inhibition;⁴³ making SKN-1/Nrf a possible therapeutic target for increasing the efficacy of proteasome inhibitors. Genes regulated by SKN-1 as part of the ER stress response includes many of the core UPR components, such as *ire-1*, *xbp-1*, *hsp-4*, *aft-5* and in fact also includes feed-forward expression of *skn-1* itself.⁴⁴

The relationship between SKN-1 and the UPR_{ER} is further complicated by the role of the UPR_{ER} regulating SKN-1 activity in response to stress. Under oxidative stress conditions, UPR_{ER} factors such as IRE-1 or HSP-4 are actually required for SKN-1 to actively regulate downstream target genes.⁴⁴ It is also known that SKN-1 is constitutively present in the nucleus in low levels even during non-stressed conditions,⁴⁵ this may suggest that SKN-1 activity may be in-part controlled by association with cooperative or inhibitory factors that are regulated by processes such as the UPR_{ER}; however this is unclear.

1.2.4 Mitochondria and energy balance

Mitochondria are dynamic organelles that have the potential to form large tubular networks under the control of fission, fusion and mitophagy. The regulation of mitochondrial network structures in order to maintain homeostatic balance is called mitohormesis. This response is induced by the onset of redox stress by reactive oxygen species (ROS) or energy imbalance, and results in the induction of cellular cues such as the mitochondrial UPR (UPR_{mt}), mitophagy, dynamic remodelling and mitokine release. The link between healthy mitochondrial ageing and longevity is best described in the mitochondrial free radical theory of ageing (MFRTA) which suggests that damage to macromolecules by ROS produced during oxidative stress strongly contributes to cellular and organismal ageing.⁴⁶ Gaining a better understanding of the process of functional decline in mitochondria during ageing also has a large number of

medical applications including mitochondrial disease, cancer, inflammatory disease, neuropathy and neurodegenerative disease.

Maintenance of mitochondrial network homeostasis through dynamic remodelling, fission and fusion, is required for intermittent fasting-induced longevity effects in *C. elegans*. This is dependent on AMPK, fatty-acid oxidation (FAO) and peroxisomal activity. Inhibition of fission or fusion reduces AMPK activity and blocks DR-induced longevity; however, co-inhibition of both fission and fusion can extend lifespan through maintenance of healthy mitochondrial structure without dynamic remodelling.⁴⁷ AMPK is a central regulator of cell energy homeostasis through its role in metabolic signalling, stress and responsiveness to AMP. In addition to this, AMPK controls mitohormesis by inducing biogenesis, dynamic remodelling and mitophagy/autophagy through PGC1 α , DRP1 and ULK1 respectively, and also exerts this function through inhibition of the mTORC1 complex (Figure 4).⁴⁸

Impairment of mitophagy causes an accumulation of functionally aberrant mitochondria, and compromises stress resistance; resulting in the induction of a retrograde oxidative stress signal that is dependent on SKN-1. SKN-1 has the role of regulating mitochondrial biogenesis as well as feed-forward signalling through DCT-1 to enhance mitophagy. In *skn-1* knockout experiments expression of *dct-1* is reduced, and therefore also the mitophagy response is impaired.⁴⁹ In this way, SKN-1 is linked to the classical mitophagy pathway and is probably involved in the maintenance of healthy mitochondria during ageing.

Experiments with SKN-1 knockdown *C. elegans* have also shown that the lack of SKN-1 changes mitochondrial network morphology in the body wall muscle cells of adult worms. Genetic mutants of *skn-1* can induce mitochondrial membrane depolarisation, increased cytoplasmic Ca²⁺ and reduced total mtDNA.⁴⁹ Low levels of insulin will induce mitophagy but not in *skn-1* mutant worms, and knockdown combinations of *skn-1*, *daf-16* and *dct-1* will not produce any more of a significant effect of single knockdowns; suggesting that these molecules contribute to mitophagy as part of a common pathway.⁴⁹

Mutations affecting *skn-1* gain of function alleles also results in a permanently active starvation response that is dependent on SKN-1. Canonical SKN-1 regulation by the IIS is independent of this starvation response, and the response is instead dependent on the association of SKN-1 with mitochondrial outer membrane protein PGAM-5.⁵⁰ In addition to this, mutations in *skn-1* gain of function alleles also induce a *Sma* phenotype (small body size) which is attributed to reduced production of ATP during development.⁵⁰

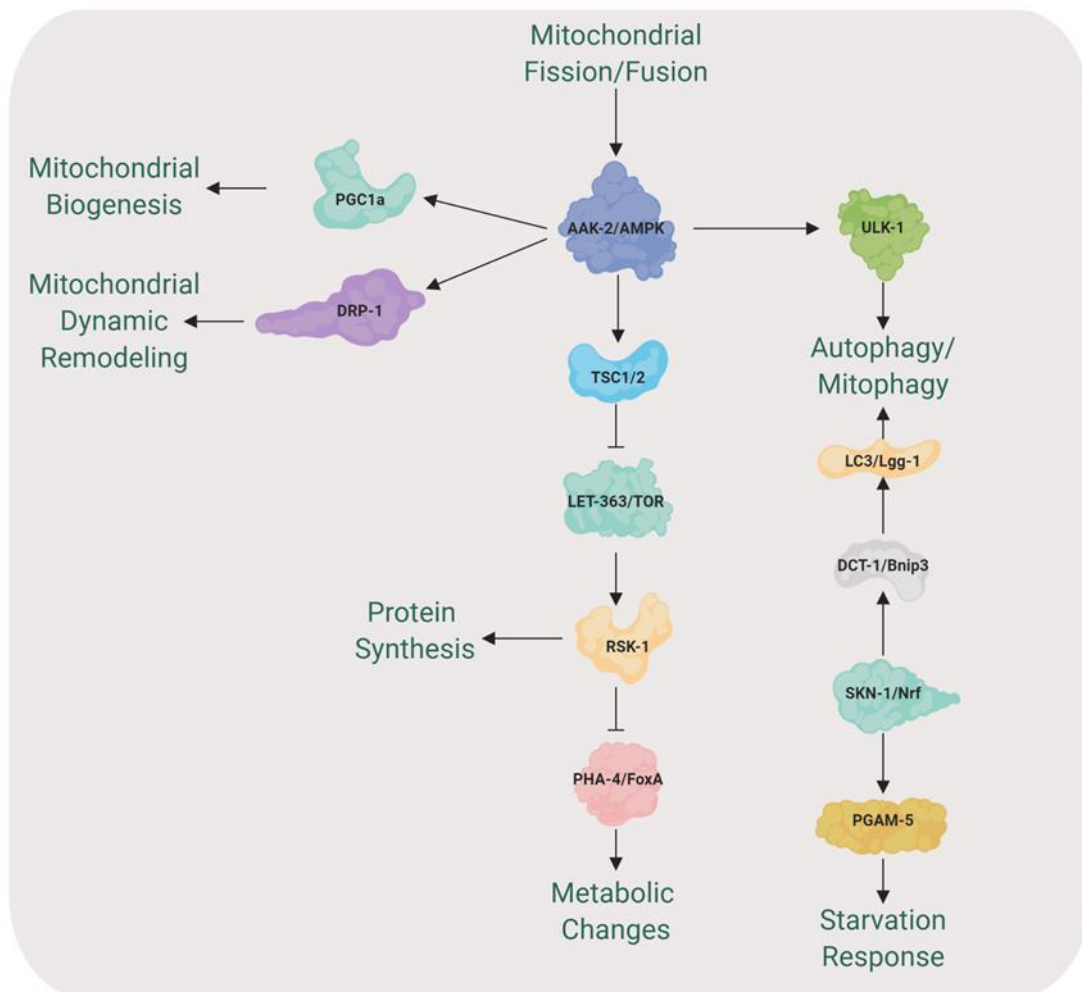


Figure 4 – Mitochondrial signalling pathways in *C. elegans*

The core regulatory molecule for mitochondrial homeostasis is AMPK, which controls signalling axes resulting in biogenesis, dynamic remodelling and fission/fusion of mitochondria. SKN-1 also has a role in mitochondrial function by direct association with PGAM-5 to orchestrate a unique starvation response,⁵⁰ and via DCT-1/Bnip3 to regulate mitophagy.⁴⁹ Image created using BioRender. Signalling information obtained from KEGG.

Together, this evidence suggests that SKN-1 has an important yet not fully defined role in regulating the biogenesis, activity, lifespan and morphology of mitochondria in *C. elegans*. Of particular interest to this study, it is unclear whether neuronal SKN-1B has any influence on the regulation of mitochondrial networks by fission, fusion or mitophagy. However, the role of SKN-1B in tissue coordination via ILP to IIS signalling may suggest that SKN-1B could also have a role here; as the IIS in body wall muscle is important for orchestrating appropriate morphological changes to mitochondrial networks in response to redox and energy imbalance.

1.4 Research aims

The aim of this study is to investigate the effects of the specific *skn-1b(tm4241)* loss-of-function mutation on three main pathways that are known to influence longevity: IIS, UPR_{ER} and mitochondrial network morphology. As DR has been shown to be important for these pathways, and to be associated to the ASI neurons (and therefore possibly SKN-1B), these effects will be investigated also in the context of DR (IDR and BD) to identify novel points of regulation for SKN-1B that may be involved in improving lifespan or age-related health. To this end, we have implemented the use of a truncated form of SKN-1B (*tm4241* mutation) which results in expression of a non-functional SKN-1B product that is likely degraded by proteasomal machinery. We have also put to use a *SKN-1B::GFP* transgenic strain that specifically overexpresses GFP-tagged SKN-1B; because SKN-1B is epigenetically regulated to be expressed independently in the ASI neurons, this results in a specific GFP signal originating in the ASIs. This tool will be used to assess changes in SKN-1B expression as a consequence of manipulation of other signalling pathways or genes.

2. Materials and methods

2.1 Strains

Table 2 – List of *C. elegans* strains used

Strains JMT82, JMT85 and JMT76 were produced as part of this study, as detailed in sections 2.3.2, 2.3.3 and supplementary figures 1-4. All other strains were gifted by Dr. Jennifer Tullet at the University of Kent.

Name	Genotype
CGCM	N2 wildtype
GA1058	<i>skn-1b(tm4241) IV</i>
GA1017	<i>wuEx217[skn-1b::GFP::skn-1 3'UTR]</i>
GA1064	<i>muEx227[pNL213(<i>ges-1p::GFP::daf-16</i>) + <i>rol-6(su1006)</i>]</i>
GA400	<i>wuEx43[pPD95.77 <i>sod-3::GFP</i>, <i>rol-6(su1006)</i>]</i>
SJ4005	<i>zcls4[hsp-4::GFP] V</i>
WBM671	<i>wbmEx289[myo-3p::tomm20(aa1-49)::GFP::unc54 3'UTR]</i>
JMT82	<i>muEx227[pNL213(<i>ges-1p::GFP::daf-16</i>) + <i>rol-6(su1006)</i>]; <i>skn-1b(tm4241) IV</i></i>
JMT85	<i>wuEx43[pPD95.77 <i>sod-3::GFP</i>, <i>rol-6(su1006)</i>]; <i>skn-1b(tm4241) IV</i></i>
JMT80	<i>zcls4[hsp-4::GFP] V; <i>skn-1b(tm4241) IV</i></i>
JMT76	<i>WbmEx289[myo-3p::tomm20(aa1-49)::GFP::unc54 3'UTR]; <i>skn-1b(tm4241) IV</i></i>

2.2 List of reagents

Nematode growth medium (NGM)

0.3% NaCl w/v, 1.7% granulated agar w/v, 0.25% bactopectone w/v in dH₂O autoclaved and cooled before addition of sterile 25mM KH₂PO₄ pH6.0, 1mM MgSO₄, 1mM CaCl₂ and 5µgm/mL cholesterol in ethanol.

M9 buffer

0.3% KH₂PO₄ w/v, 0.6% Na₂HPO₄ w/v, 0.5% NaCl w/v in dH₂O autoclaved and cooled before addition of sterile 1mM MgSO₄.

LB plates and media

LB agar was produced by adding 2.5% LB broth w/v and 1.5% granulated agar w/v in dH₂O and sterilised by autoclave.

LB liquid media was produced by adding 2.5% LB broth w/v in dH₂O and sterilised by autoclave.

Antibiotics were added where necessary after sterilisation; see sections 2.3.2 and 2.3.4 for OP50-1 and HT115 *E. coli* cultures respectively.

IDR dietary restriction medium

This DR protocol requires two phases, a bottom solid agar mix and an aqueous layer above to hold worms in suspension. This was performed in 6 or 24-well plates, with equal volumes of top and bottom IDR media used (2.5mL in 6-well plates, 500µL in 24-well plates).

IDR bottom media contains the standard NGM mix with the addition of 1mg/mL erythromycin, 12.5µg/mL FuDR, 50µg/mL ampicillin and 1mM IPTG. IDR top media contains the same preparation with the omission of agar from the NGM mix.

2.3 Methods

2.3.1 Bacterial cultures

Bacterial cultures stored in 50% glycerol in dH₂O at -80°C were used to obtain single cell colonies on LB agar by streaking and incubating overnight at 37°C. Single colonies obtained from LB agar plates were used to inoculate LB liquid medium and grown overnight at 37°C with agitation.

Where necessary, antibiotics and accessory components were added to media for selection or gene induction (see sections 2.3.2 and 2.3.4 for OP50-1 and HT115 respectively).

2.3.2 Animal husbandry

C. elegans strains were grown on NGM plates seeded with OP50-1 *E. coli* and unless otherwise stated were grown at 20°C. In LB agar plates, NGM plates and LB liquid media 200µg/mL streptomycin and 10µg/mL nystatin were added for selection. Before experiments

were carried out, worms were fed ad libitum for at least 3 generations prior in order to restore epigenetic changes as a result of reduced food availability.

Induction of males for genetic crosses was carried out by heat shock of L4 stage worms at 30°C for 5 hours. Males were then identified by eye and used to create male stock plates. For crosses, L4 stage worms were placed onto a small spot of OP50-1 on an otherwise empty NGM plate at a ratio of 1:7 hermaphrodites-to-males in order to ensure a high probability of male fertilisation. After the initial cross, F1 generation worms were individually transferred onto new seeded NGM plates and clonal F2 generation worms were genotyped.

Rolling worms (*rol-6 (su1006)*) where used were identified by eye. This transgenic strain expresses a defective cuticle component which results in the unilateral movement of the worm in circles (rolling) opposed to its usual sinusoidal movement and so therefore is a very useful tool in tracking transgene inheritance.

2.3.3 Strain validation (genotyping)

Individual F2 generation worms were dropped into 5µL worm lysis buffer (50mM KCl, 10mM Tris-HCl pH8.3, 2.5mM MgCl₂, 0.45% NP-40, 0.45% Tween-20, 0.01% Gelatin, 1mg/mL Proteinase K) inside PCR tube lids before replacing the bottom of the tubes, centrifuging and starting lysis (70°C/1hr, 95°C/15min, 10°C/∞).

After lysis and centrifugation, 15µL of PCR mastermix (2µM of each forward, reverse and internal primer in GoTaq all-in-one in dH₂O) was added to each of the 5µL of lysed worms before PCR (94°C/1min, [94°C/30s, 60°C/30s, 72°C/1min]x30, 72°C/7min, 10°C/∞).

The 20µL of PCR preparation was then transferred to a 1% agarose gel stained with ethidium bromide for visualisation.

2.3.4 RNAi

For RNAi, worms were grown on NGM plates containing 25µg/mL ampicillin and 1mM IPTG seeded with HT115 *E. coli* in LB liquid media also containing 25µg/mL ampicillin and

12.5µg/mL tetracycline. HT115 used for inoculation was grown on LB agar containing 25µg/mL ampicillin for selection.

The HT115 strains used expressed complementary dsDNA to target genes inducible by IPTG; after seeding, plates were left for at least 24 hours to allow induction of dsDNA before transfer of worms for feeding.

2.3.5 Lifespan analysis

Worms at L4 stage were picked from OP50-1 seeded NGM plates and transferred onto fresh plates seeded with either HT115 or OP50-1 depending on whether RNAi would be used (see section 2.3.4 for RNAi), with additional 12.5µg/mL FuDR pipetted directly on-top of the bacterial lawn to limit progeny hatching. 20 worms were transferred per lifespan plate to improve accuracy of counting (5 plates per lifespan).

Worms were scored every second day for the numbers alive, dead and censored. Censored worms include those killed by transfer, escaping the plate, burrowing, exploding intestine, internally hatched progeny, vulvar protrusion or contamination. Incubation temperature unless otherwise stated was 20°C.

Lifespan analysis was carried out using OASIS 2.

2.3.6 Dietary restriction

Bacterial deprivation (BD) was carried out by transfer of L4-stage worms to empty NGM plated without any food source for 16 hours prior to analysis. Worms were previously grown on OP50-1 seeded NGM for at least 3 generations prior to transfer.

Liquid DR (IDR) was carried out by transferring L4-stage worms to solid IDR NGM inside 6 or 24-well plates before addition of IDR top media (see section 2.2) containing HT115 PL4440 empty-vector *E. coli*. LB liquid culture of HT115 was centrifuged at 5000rpm for 2 minutes, media was discarded, and the pellet was resuspended in IDR top media. Dilutions were

calculated by measurement of OD at 600nm to create a series of 2.5×10^9 CFU/mL, 1.25×10^9 CFU/mL, 2.5×10^8 CFU/mL, 2.5×10^7 CFU/mL 2.5×10^6 CFU/mL and 0 CFU/mL.

2.4 Microscopy

2.4.1 Fluorescence

Glass slides were prepared by placing a drop of 3% molten agarose in water onto a slide and then sandwiching another slide on-top using two adjacent taped slides as spacers to produce a thin agarose pad.⁵¹ Worms were then immobilised on agarose pads in a drop of $\sim 10 \mu\text{L}$ 0.01% tetramisole hydrochloride in M9 with a glass cover slip placed on top.

Images were acquired on a CCD camera using Leica Microsystems LAX X Life Sciences software. Exposure times varied between experiments as indicated in results. Image analysis was carried out by export of images to Fiji (ImageJ). Regions of interest were drawn (varying between experiment, e.g. whole worm or neuronal) and mean grey values were obtained to represent fluorescence intensity.

2.4.2 TEM

A large number of L4 worms (~ 100 - 200) were selected and transferred to M9 suspension in a 100mm x 15mm culture dish. The M9 was aspirated and replaced by 2mL 2.5% glutaraldehyde in 100mM sodium cacodylate (CAB) buffer pH7.2. Under a dissecting scope in a fume hood, heads and tails of the worms were removed with a fresh scalpel; dissected worms were left overnight in the fixative at 4°C.

Worms were washed twice with CAB and suspended in 2% low melting point agarose in CAB. Agarose was placed briefly at 4°C to solidify. Worms were identified under the microscope, excised and transferred in agarose to 7mL glass vials where they were post-fixed in 1% osmium tetroxide in CAB for 1 hour at room temperature. Samples were washed twice in Milli-Q water for 10 minutes, then dehydrated in an ethanol series of 50%, 70%, 90% and finally

100% dry ethanol for 10 minutes each. The samples were then washed twice for 10 minutes each in propylene oxide.

Freshly prepared agar scientific low viscosity (LV) resin was prepared fresh and mixed 1:1 with propylene oxide before addition to the samples for 30 minutes at room temperature. Samples were incubated in fresh LV resin twice for 2 hours each. Samples were finally embedded in LV resin in shallow aluminium dishes and polymerised at 60°C for 24 hours. After polymerisation, worm fragments were identified by dissecting scope and individual worms were excised and orientated on a resin block for optimal sectioning.

Sections of 70nm were cut using a Leica EM UC7 ultramicrotome with a Diatome diamond knife and collected onto 400-mesh copper grids (Agar Scientific). Counterstaining of sections was carried out by placing grids into droplets of 4.5% uranyl acetate for 45 minutes and Reynolds lead citrate for 7 minutes.

2.5 Statistics

For multiple comparisons across a single group, a simple Dunnett corrected One-Way ANOVA was used; and for multiple comparisons of multiple groups, a Sidak corrected Two-Way ANOVA ($\alpha=0.05$) was used. Significance was reported as: ns = $P>0.1234$, * = $P<0.0332$, ** = $P<0.0021$, *** = $P<0.0002$, **** = $P<0.0001$.

When comparing the distributions of graded results (those of a pre-determined/categorical scale, used in DAF-16 analysis), the Chi Square test was used. To compare survival distributions during lifespan analyses, a long-rank test was used to determine changes of statistical significance. Significance here was reported as: ns = $P>0.05$, * = $P<0.05$, ** = $P<0.001$, *** = $P<0.0001$,

Results

The aim of this study was to interrogate the role of SKN-1B within three distinct organismal processes which have all been linked to the regulation of lifespan. These processes are also affected by energy balance and exogenous cues such as sensory perception of food sources. As SKN-1B is uniquely expressed in the chemosensory ASI neurons, this point of regulation was investigated by bacterial deprivation or dilution in comparison to worms fed ad libitum.

In order to achieve these goals, genetic crosses were first carried out to introduce the *skn-1b(tm4241)* mutation, hereby referred to as $\Delta skn-1b$, into GFP reporter strains. This included the generation of JMT76, JMT82 and JMT85. Identification of successful crosses was carried out by visual confirmation of GFP or rolling phenotypes of reporter genes in addition to PCR amplification of the $\Delta skn-1b$ mutation site using a 3-primer strategy to identify homozygous mutant $\Delta skn-1b$ worms as summarised in supplementary figures 1-4.

3.1 *skn-1b::GFP* expression is increased by dietary restriction

To better understand the effects of reduced food intake on *skn-1b* expression, worms fed ad libitum on OP50-1 *E. coli* were placed on empty NGM plates (BD) for a period of 16 hours at 20°C prior to immobilisation on glass slides and imaging of *skn-1b::GFP* (Figure 5A/C) in the ASI neurons. After starvation, these worms showed a significant increase in *skn-1b::GFP* fluorescence intensity at 200msec exposure to ~1.5-fold of the fed control group ($P < 0.0001$, $N \geq 135$).

In addition to bacterial deprivation, dilution of bacteria had a dose-dependent effect on *skn-1b::GFP* expression. Here, worms were placed into suspension of HT115 *E. coli* of a pre-determined CFU/mL value in a 24 well plate, in a protocol adapted from Bishop *et. al.*⁷ Worms were incubated at 20°C for 16 hours in IDR plates before being taken for imaging, exposure here was also 200msec. Induction of *skn-1b::GFP* rose significantly to a similar level as BD and peaked at 2.5×10^7 CFU/mL ($P < 0.0001$, $N \geq 80$) (Figure 5B/D), showing that near-starvation conditions induce *skn-1b::GFP* to higher levels than complete bacterial deprivation. During

starvation also, it was observed that *skn-1b::GFP* was stably expressed in two or more additional neurons very close to the ASI neurons with an unknown function (data not shown). The frequency of these observations was also highest at 2.5×10^7 CFU/mL, which could suggest an unknown function of SKN-1B in these additional neurons that is controlled by a low sensory threshold possibly originating in the ASIs. Raw data for *skn-1b::GFP* fluorescence in BD and IDR protocols can be seen in supplementary figures 5 and 6 respectively.

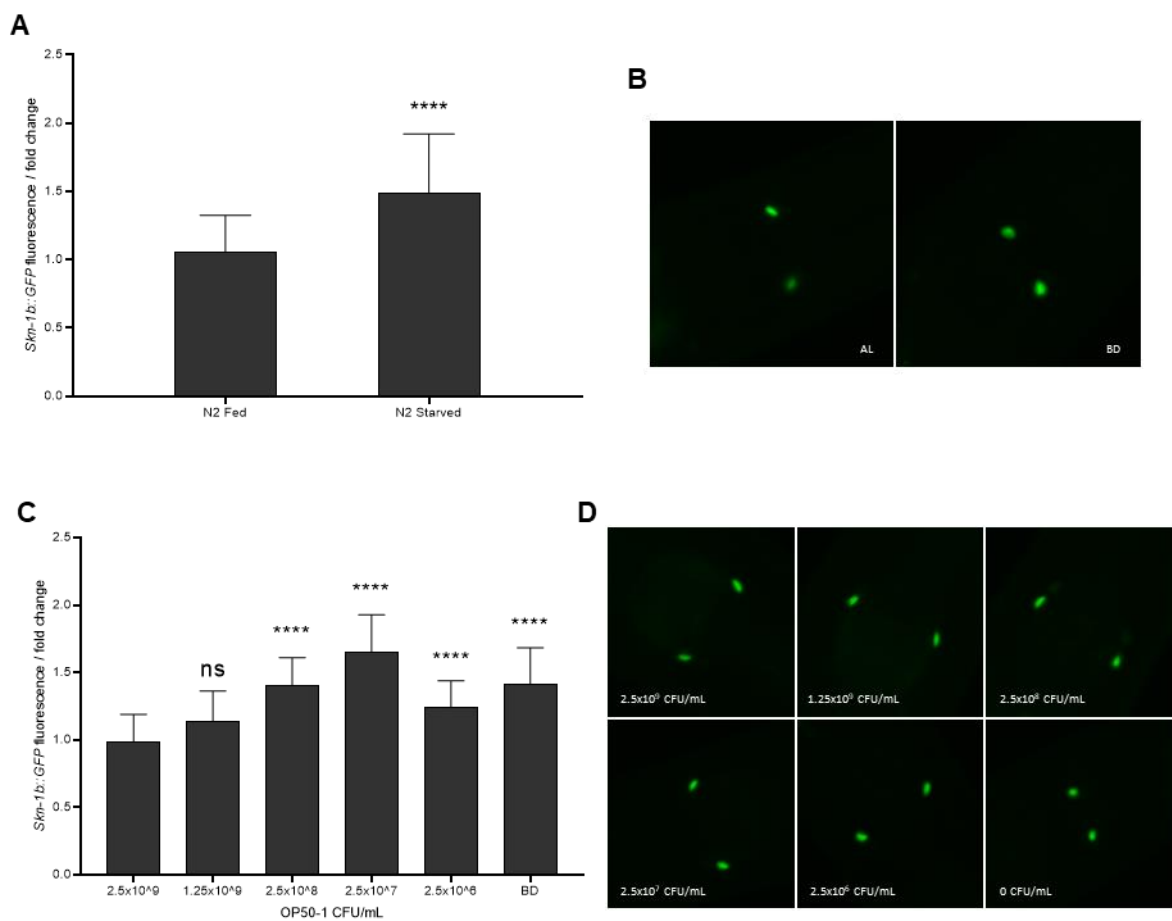


Figure 5 – Expression of *skn-1b::GFP* in response to dietary restriction by bacterial deprivation.

ASI specific expression of SKN-1B was measured by GFP signal in response to dietary restriction by bacterial deprivation (A,B) or bacterial dilution (C,D). All data is representative of at least 3 replicates. Error bars show standard deviation of the mean. [(A), (B) Obtained from Dr. Max Thompson]. ns = $P > 0.1234$, * = $P < 0.0332$, ** = $P < 0.0021$, *** = $P < 0.0002$, **** = $P < 0.0001$.

3.2 DR-induced nuclear DAF-16 is short-lived in $\Delta skn-1b$ mutant worms

SKN-1 acts in parallel to DAF-16 downstream of the IIS signalling axis, and it is known that ASI-specific SKN-1B contributes to the expression of peptide signalling intermediates such as *ins-7* that feed into the IIS in other tissues (data not shown). Therefore, it was next investigated whether SKN-1B is required for intestinal DAF-16 localisation and expression in the context of dietary restriction. To this end, a grading system was implemented to assess the level of nuclear localisation and expression of intestinal DAF-16::GFP shown in figure 6D and figure 6E respectively.

Daf-16::GFP N2 and $\Delta skn-1b$ worms fed ad libitum on OP50-1 culture were transferred to empty NGM plates for 16 hours at 20°C for BD; imaging whole worms at 300msec exposure was carried both before and after (3 and 6 hours) re-feeding. Other studies have shown that re-feeding of worms induces a quiescent behavioural state that is dependent on DAF-16 activity that normalises within 24 hours of re-feeding.³⁷ Here, we observed an induction of intestinal DAF-16 nuclear localisation (Figure 6A) and expression levels (Figure 6B) that remained consistent after 6 hours of re-feeding in N2 worms ($P < 0.0001$, $N \geq 59$; $P < 0.0001$, $N \geq 59$); however, this phenotype was short-lived in $\Delta skn-1b$ worms which converged towards basal *daf-16::GFP* localisation/expression within 3 hours ($P < 0.0001$, $N \geq 53$; $P < 0.0001$, $N \geq 53$).

Next, N2 and $\Delta skn-1b$ worms were also transferred to liquid suspension of HT115 *E. coli* at different dilutions for 16 hours at 20°C for IDR. Dietary restriction by bacterial dilution also induced intestinal *daf-16::GFP* nuclear localisation in a dose-dependent manner ($P < 0.0001$, $N \geq 51$), although this was independent of $\Delta skn-1b$ ($P > 0.05$, $N \geq 51$) (Figure 6C). The percentage distributions of graded worms can also be seen in supplementary figure 7. Raw data for BD and IDR methods of DR are shown in supplementary figures 8 and 9 respectively.

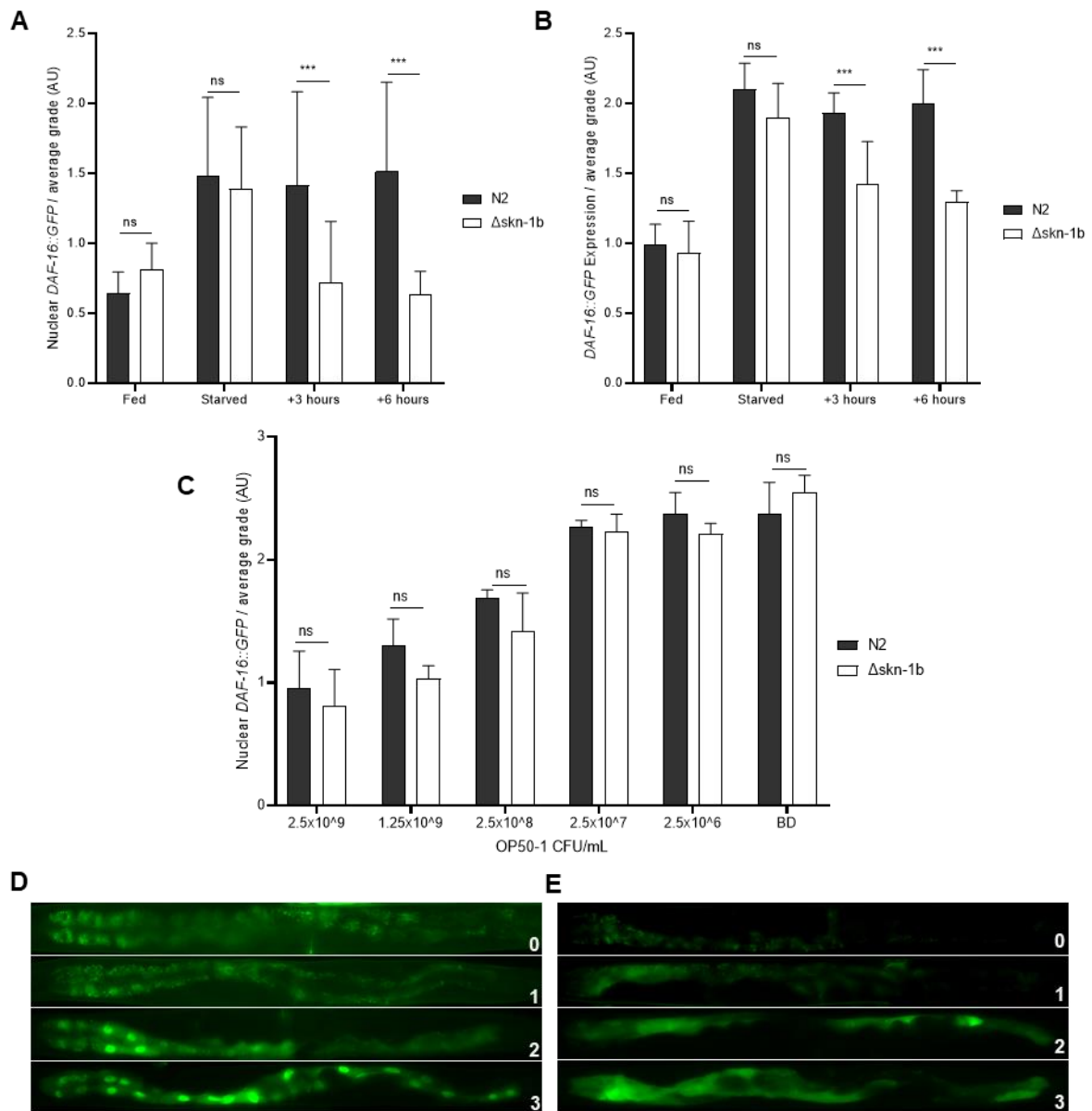


Figure 6 – *Daf-16::GFP* expression in response to starvation in *N2* and $\Delta skn-1b$ worms

Nuclear localisation and expression of *Daf-16::GFP* was determined after bacterial deprivation (A,B) and nuclear localisation after bacterial dilution (C) by a 4-point grading system (D,E). All data is representative of at least 3 biological replicates, error bars show standard deviation of the mean. ns = $P > 0.05$, * = $P < 0.05$, ** = $P < 0.001$, *** = $P < 0.0001$,

3.3 IDR, but not BD, demonstrates SKN-1B-dependent *sod-3::GFP* upregulation

As the DAF-16 data in section 3.2 explores localisation and expression levels of DAF-16 but not transcriptional activity, it was next asked whether SKN-1B is required for the transcriptional effects of DAF-16. To this end, a *sod-3::GFP* reporter strain was used to assess whole-worm fluorescence in BD and IDR contexts as a readout for DAF-16 activity.

N2 and $\Delta skn-1b$ worms grown ad libitum were transferred onto empty NGM plates for 16 hours at 20°C to induce DR by BD. Fluorescence intensity in whole worms at 150msec was measured and showed a ~2-fold increase in *sod-3::GFP* expression after BD in both N2 and $\Delta skn-1b$ worms ($P < 0.0001$, $N \geq 57$; $P < 0.0001$, $N \geq 59$). There was no significant difference between N2 and $\Delta skn-1b$ worms in either fed or starved conditions, indicating that SKN-1B is not required in this context for DAF-16 transcriptional activity in regulating *sod-3* ($P > 0.05$, $N \geq 59$; $P > 0.05$, $N \geq 57$) (Figure 7A/C).

Next, N2 and $\Delta skn-1b$ worms were placed in IDR plates for 16-hours at 20°C prior to imaging also at 150msec. Expression of *sod-3::GFP* was also induced by IDR in N2 worms ($P < 0.0001$, $N \geq 57$), but not in $\Delta skn-1b$ worms ($P > 0.05$, $N \geq 57$) (Figure 7B/D). As $\Delta skn-1b$ worms showed a significantly lower expression of *sod-3::GFP* by IDR ($P < 0.0001$, $N \geq 57$), it can be assumed that SKN-1B may be required for DAF-16 activity in this context at least for appropriate expression of *sod-3*. Additionally, the induction of *sod-3::GFP* by IDR was much lower than the degree seen by BD (~1.3-fold vs. ~2-fold). It is unclear why this difference occurs, and as previously discussed this may be due to perceptual differences in a liquid vs. solid food source. Nevertheless, the IDR method has previously been shown to require SKN-1B for longevity effects and it may be beneficial to fully elucidate the specific context requirements for SKN-1B dependency. Raw data for *sod-3::GFP* BD and IDR experiments can be seen in supplementary figures 10 and 11.

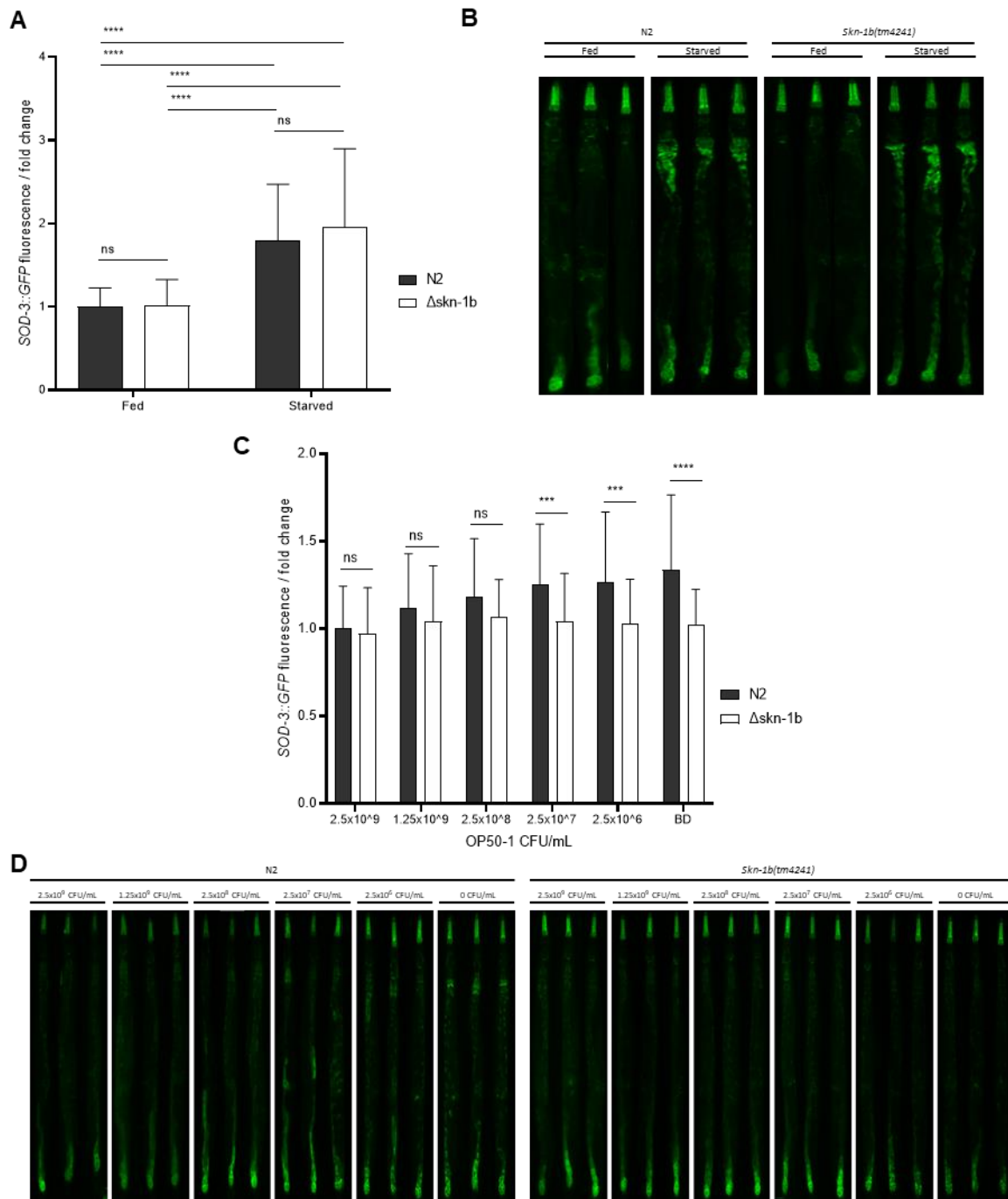


Figure 7 – *Sod-3::GFP* expression in response to starvation in N2 and $\Delta skn-1b$ worms

Expression of *Sod-3::GFP* was determined by whole-worm fluorescence in N2 and SKN-1B mutant backgrounds after bacterial deprivation (A,B) or bacterial dilution (C,D). All data is representative of at least 3 biological replicates, error bars show standard deviation of the mean. ns = $P > 0.1234$, * = $P < 0.0332$, ** = $P < 0.0021$, *** = $P < 0.0002$, **** = $P < 0.0001$.

3.4 SKN-1B may be required for UPR_{ER} component expression but not induction

The next pathway investigated was the UPR_{ER} which couples longevity to enhanced stress resistance and complex changes to translational networks that are still not fully understood. Within this pathway, SKN-1 has a role in the transcriptional regulation of several UPR_{ER} components including HSP-4. Here, we look to see whether neuronal SKN-1B is required for distal tissue expression or induction of the abundant HSP-4 chaperone protein.

Hsp-4::GFP worms in N2 and $\Delta skn-1b$ backgrounds fed ad libitum on OP50-1 culture were starved for 16 hours at 20°C on empty NGM plates (BD) prior to imaging at 200msec exposure. In fed conditions, $\Delta skn-1b$ worms had a significantly reduced *hsp-4::GFP* expression when compared to the N2 control group ($P < 0.0001$, $N \geq 62$) suggesting that SKN-1B could be required for proper basal expression levels of *hsp-4* and positively regulates *hsp-4* expression in normal conditions. Additionally, starvation reduces expression of *hsp-4::GFP* in N2 worms with a further reduction in $\Delta skn-1b$ worms ($P < 0.0001$, $N \geq 63$; $P < 0.0001$, $N \geq 65$) (Figure 8A/C). This may be reflective of a reduced UPR_{ER} response in $\Delta skn-1b$ worms, or may be a transcriptional affect as *hsp-4* is a SKN-1 target gene.

Next, we wanted to demonstrate that *hsp-4::GFP* expression is reflective of the UPR_{ER} activity in this context. It is known that RNAi of the *ero-1* oxidase will truncate the ERAD and induce UPR_{ER} activity due to accumulation of misfolded protein, and this should likewise induce UPR_{ER} components such as *hsp-4*. For this, N2 and $\Delta skn-1b$ worms were grown on HT115 *ero-1* RNAi plates for 24 hours prior to imaging. It was successfully demonstrated that *ero-1* RNAi strongly induced *hsp-4::GFP* expression to ~6-fold the basal level in N2 and $\Delta skn-1b$ worms ($P < 0.0001$, $N \geq 54$; $P < 0.0001$, $N \geq 56$) with no significant difference between N2 and $\Delta skn-1b$ during *ero-1* RNAi ($P > 0.05$, $N \geq 56$) (Figure 8B/D). This suggests that whereas SKN-1B may be required for expression of *hsp-4* in normal conditions, it is not required for the induction of *hsp-4* in response to ER stress. Raw data for *hsp-4::GFP* BD and *ero-1* RNAi can be found in supplementary figures 12 and 13 respectively.

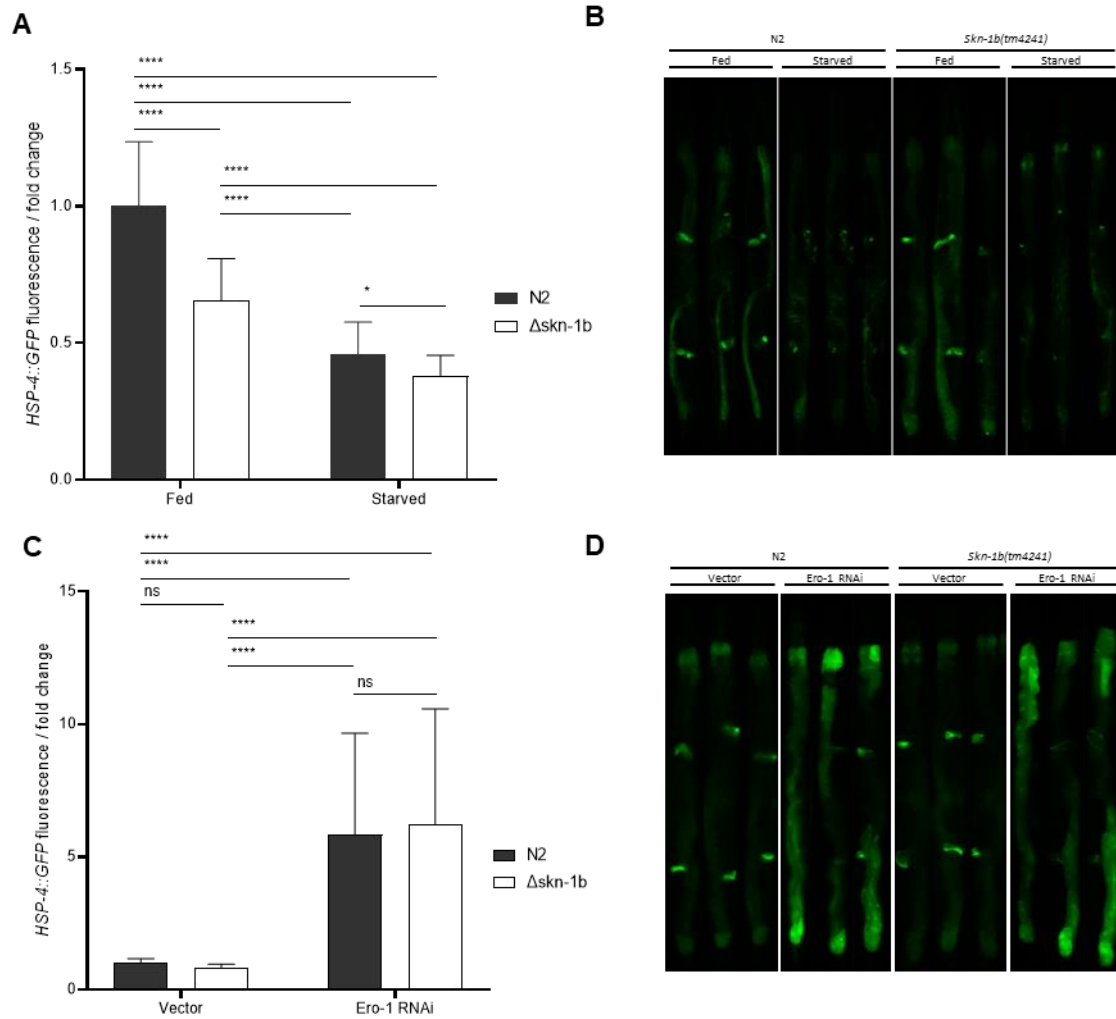


Figure 8 – Expression of *hsp-4::GFP* after starvation and *ero-1 RNAi*

Expression of *Hsp-4::GFP* was measured by whole-worm fluorescence in N2 and SKN-1B mutant worms following bacterial deprivation (A,B) and *ero-1 RNAi* to induce the UPR_{ER} (C,D). All data is representative of at least 3 biological replicates, error bars show standard deviation of the mean. ns = $P > 0.1234$, * = $P < 0.0332$, ** = $P < 0.0021$, *** = $P < 0.0002$, **** = $P < 0.0001$.

3.5 SKN-1B is not required for the *ero-1* longevity phenotype

In addition to *ero-1* RNAi inducing the UPR_{ER}, as part of this phenotype it also has pro-longevity effects that are dependent on UPR_{ER} signalling pathways. To investigate whether SKN-1B is required for this phenotype, we conducted a lifespan experiment; where a population of worms are monitored over their lifetime and the number of dead, surviving and censored (those that have died from unnatural causes) animals are recorded.

First though, we wanted to investigate whether *ero-1* RNAi had any effect on SKN-1B expression itself. For this, *skn-1b::GFP* worms were grown on RNAi plates containing either control vector or *ero-1* vector HT115 *E. coli*. These were grown for 24 hours at 20°C prior to imaging at 200msec exposure. It was found that *ero-1* modestly increased *skn-1b::GFP* expression to a significant level ($P < 0.05$, $N \geq 55$) (Figure 9A), suggesting that *ero-1* RNAi may have some unknown SKN-1B-dependent effects. Although, this increase is marginal and it is unclear if there is any biological significance to this change.

For lifespan analysis, N2 and $\Delta skn-1b$ worms were grown on empty vector or *ero-1* RNAi plates containing FuDR and monitored. It was observed that *ero-1* successfully prolonged lifespan in N2 worms ($P < 0.0001$, $N \geq 180$), but also in $\Delta skn-1b$ worms ($P < 0.0001$, $N \geq 180$) with no significant difference between N2 and $\Delta skn-1b$ ($P > 0.05$, $N \geq 180$); suggesting that SKN-1B is not required for *ero-1* RNAi-induced longevity (Figure 9B). There was also no difference between N2 and $\Delta skn-1b$ empty vector controls ($P > 0.05$, $N \geq 180$), showing that the $\Delta skn-1b$ mutation alone has no effect on lifespan. Raw data for *skn-1b::GFP* and lifespan analysis can be seen in supplementary figures 14 and 15 respectively.

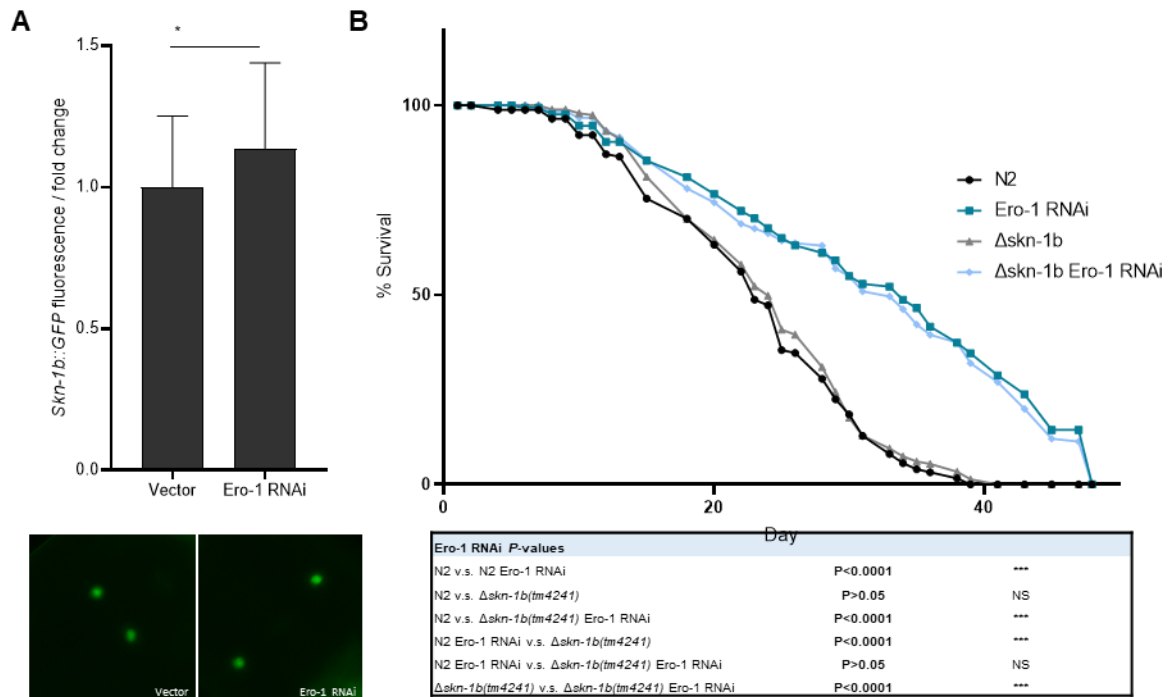


Figure 9 – *Ero-1* RNAi also induces *skn-1b::GFP* and contributes to longevity independently of *SKN-1B*

Expression of *Skn-1b::GFP* was determined by ASI fluorescence following *Ero-1* RNAi (A), and lifespan analysis of N2 and *SKN-1B* mutant worms with *Ero-1* RNAi or empty vector treatment (B). Fluorescence experiments are representative of at least biological replicated, error bars represent standard deviation of the mean. ns = P>0.1234, * = P<0.0332, ** = P<0.0021, *** = P<0.0002, **** = P<0.0001. Lifespan experiments are representative of two pooled biological replicates. ns = P>0.05, * = P<0.05, ** = P<0.001, *** = P<0.0001.

3.6 SKN-1B is important for mitochondrial morphology

Mitochondria are intimately linked to the extension of healthy organismal lifespan by the mitochondrial free radical theory of ageing (MFRTA). This theory suggests that free radicals, or reactive oxygen species (ROS) can contribute to ageing by directly damaging macromolecules. Proteins with a protective antioxidant effect can slow this process, and the overexpression of these can also contribute to extension of a healthy lifespan; SKN-1 promotes the translation of many of these antioxidant factors involved in restoring homeostasis during oxidative stress, and so we investigated the effect of the $\Delta skn-1b$ mutation on mitochondrial physiology in body wall muscles of *C. elegans*.

L4 stage worms fed ad libitum on OP50-1 *E. coli* culture were transferred to either empty or seeded NGM plates (BD) for 24 hours at 20°C prior to imaging at 400msec exposure. The largest areas of clear body wall muscle were identified between the pharynx and vulva or the vulva and the tail; no significant difference was observed between these two segments and so measurements were able to be pooled. Two measurements were taken: firstly, whole muscle fibres were isolated and a threshold was used to create a binary image where a percentage of the whole fibre covered by fluorescence could be calculated using Fiji (ImageJ), and secondly the area of each individual fluorescent object over multiple fibres from multiple worms was calculated.

In fed conditions, we observed significant decreases in the area coverage ($P < 0.0001$, $N \geq 49$) and the average area of mitochondria ($P < 0.0001$, $N \geq 518$) in $\Delta skn-1b$ worms compared to N2. Likewise, in starved conditions there was a significant drop in both coverage and area in N2 worms ($P < 0.0001$, $N = 49$; $P < 0.0001$, $N = 518$) with a further decrease in $\Delta skn-1b$ worms ($P < 0.0001$, $N \geq 49$; $P < 0.0001$, $N \geq 518$) (Figure 10A/B). Visually, the $\Delta skn-1b$ worms also had much more fragmentation in their mitochondrial networks (Figure 10C) which resembled a slightly starved phenotype more than the N2 control. Raw data for mitochondrial area coverage can be seen in supplementary figure 16.

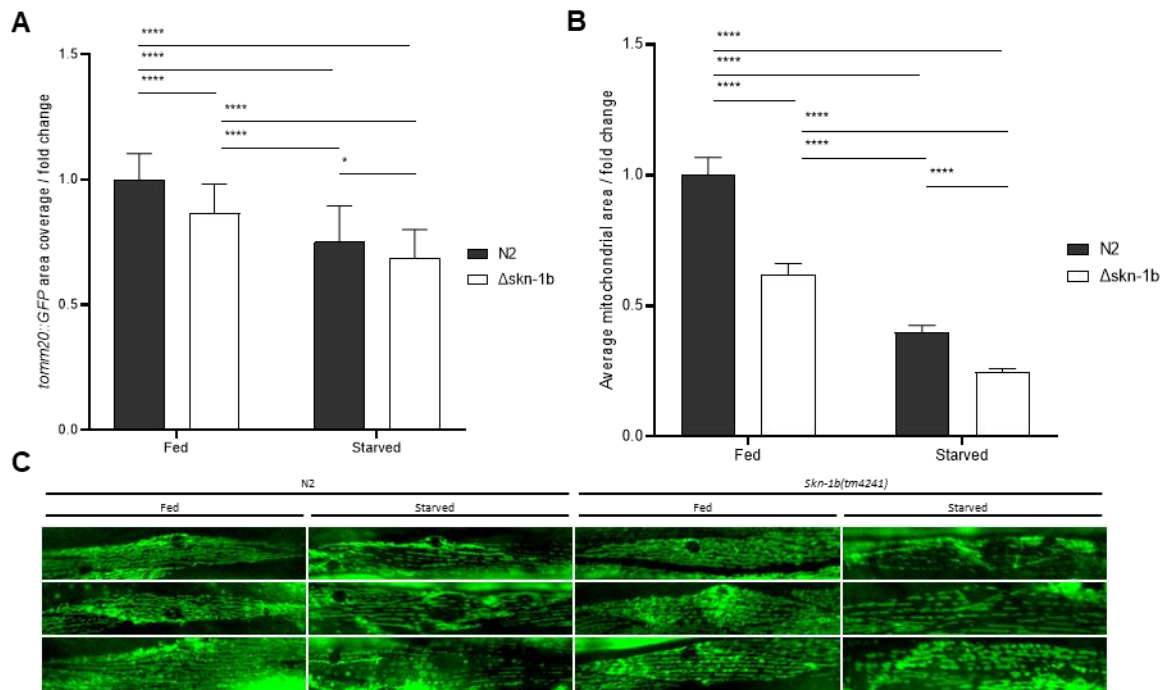


Figure 10 – Loss of SKN-1B is associated with changes in mitochondrial network morphologies

Expression of *tomm20::GFP* was used to visualise mitochondrial structures in the body wall muscle of anaesthetised worms. Average signal area coverage of whole muscle fibres (A) as well as average area of mitochondria (B) was calculated using Fiji software. Representative images of each condition shows fragmentation of networks upon starvation or SKN-1B depletion (C). Data represents at least 3 biological replicates, error bars show standard deviation of the mean. ns = $P > 0.1234$, * = $P < 0.0332$, ** = $P < 0.0021$, *** = $P < 0.0002$, **** = $P < 0.0001$.

To identify if there were any clear morphological changes to mitochondrial structures in $\Delta skn-1b$ worms, TEM images of transverse and longitudinal sections of L4 stage worms were taken in ad libitum fed conditions. In N2 worms, the mitochondria observed were firstly more numerous than $\Delta skn-1b$ mutants, possibly suggesting greater network connectivity; in addition, in $\Delta skn-1b$ longitudinal sections the mitochondria seen appeared more elongated and narrower than the N2 control (Figure 11). This data together suggests that SKN-1B may have a role in regulating mitochondrial morphology; though as the $\Delta skn-1b$ lifespan is the same as N2 wildtype, it is unclear if there is any consequence to the physiology of the worm because of this morphology change.

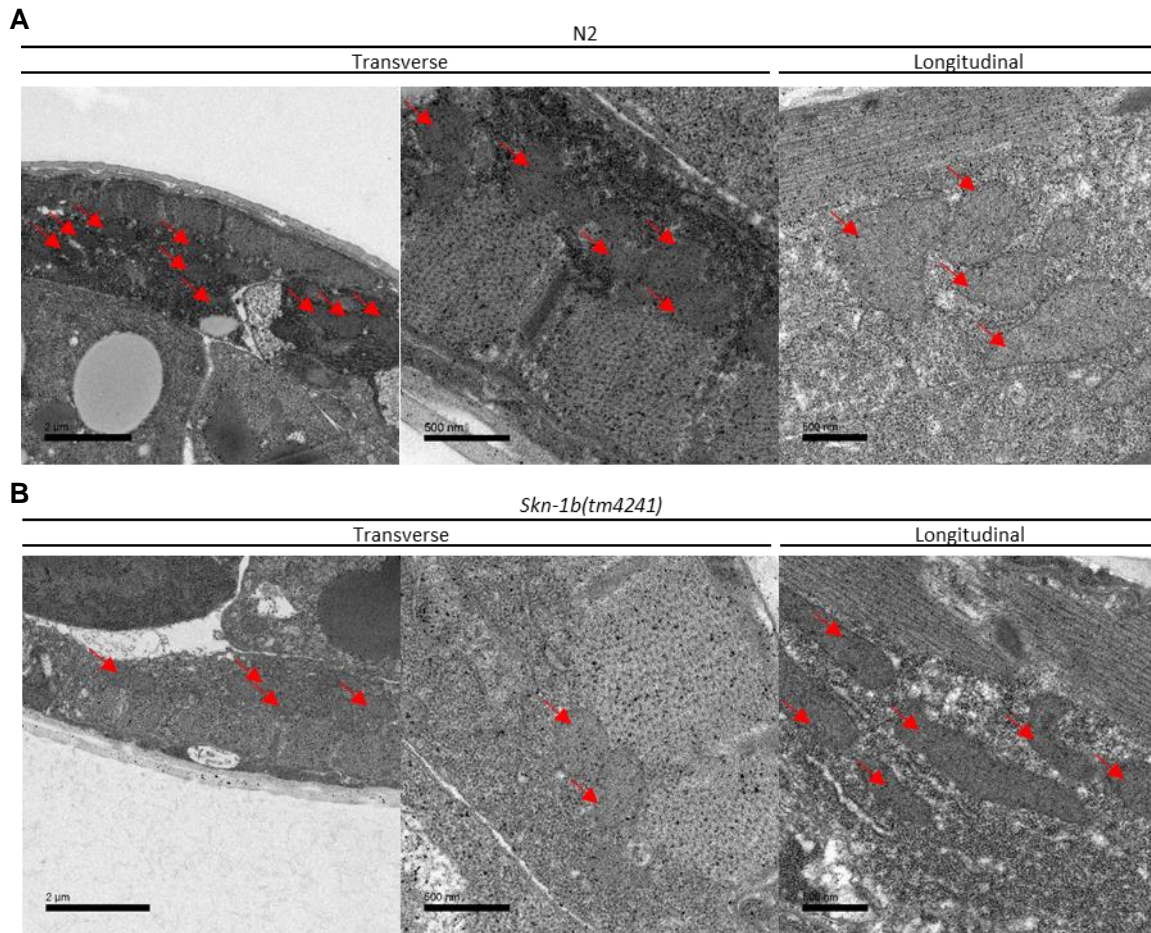


Figure 11 – TEM images of N2 and *skn-1b* worms fed ad libitum

Transverse and longitudinal sections of worms freely fed were taken and imaged to observe morphological differences in N2 (A) and $\Delta skn-1b$ (B) worms. Mitochondria are identified by red arrows. $\Delta Skn-1b$ worms were seen to have a sparser distribution of mitochondria in body wall muscle, and in longitudinal sections appeared to be more narrowed and elongated than N2 worms. Images are representative of multiple worms over one biological replicate.

Discussion

The aim of this study was to identify novel interactions of SKN-1B within three pathways involved in lifespan determination in *C. elegans* in the context of dietary restriction. From this project, it has been found that SKN-1B interacts with many branches of longevity signalling pathways in a complex and context-dependent manner that can provide insight to the function of this scarcely studied SKN-1 isoform.

4.1 Generation of new *C. elegans* strains

The first aim of this project was to produce and validate new *C. elegans* strains that were homozygous for the $\Delta skn-1b$ mutant allele and co-expressed one of the several reporter genes used here. Homozygosity of the reporter genes were identified by visual confirmation (fluorescence or rolling phenotypes) after PCR validation of the homozygous $\Delta skn-1b$ mutation using a three-primer strategy summarised in supplementary figure 1. Using this method, JMT82(*Ex[pNL213(ges-1p::GFP::daf-16) + rol-6(su1006)]; skn-1b(tm4241) IV*), JMT85(*wuEx43[pPD95.77 sod-3::GFP, rol-6(su1006)]; skn-1b(tm4241) IV*) and JMT76(*WbmEx289[myo-3p::tomm20(aa1-49)::GFP::unc54 3'UTR]; skn-1b(tm4241) IV*) were successfully produced (supplementary figure 2-4).

4.2 SKN-1B and the IIS

4.2.1 Expression of *skn-1b::GFP* is BD and IDR responsive

In this study, two individual DR protocols induced SKN-1B expression as determined by fluorescence from the *wuEx217[skn-1b::GFP::skn-1 3'UTR]* extrachromosomal array. Both BD and IDR induced *skn-1b::GFP* expression to similar levels of ~1.5-fold of the N2 wildtype control ($P < 0.0001$, $N \geq 135$, $P < 0.0001$, $N \geq 80$) (Figure 5). In addition, the appearance of additional neurons followed the same trend as *skn-1b::GFP* induction; suggesting that there may be an unknown function of SKN-1B independent of the ASI neurons that is controlled by an expression threshold (data not shown).

Both the BD and IDR protocols are able to extend lifespan, which would coincide with greater expression of SKN-1B in the ASI neurons according to this data. Although it was not investigated here whether the $\Delta skn-1b$ mutation was required for DR to extend lifespan, this would be a further consideration. The IDR protocol has been shown to require ASI-specific SKN-1B to extend lifespan, though this was performed by a *skn-1b* transgene rescue experiment in animals lacking SKN-1 (*zu135*) and may not reflect endogenous levels of SKN-1B.⁷

From the ASI neurons, although SKN-1B has been shown to be required for longevity phenotypes in the IDR method,⁷ it has not yet been investigated whether it is a requirement for BD to extend lifespan. The BD method has only been shown to extend lifespan in a manner that is dependent on neuronal DAF-7/TGF- β which, likewise, is also required for DAF-16 nuclear localisation in the intestine following DR.²⁷ However, it is known that the DAF-7/TGF- β signalling axis is also controlled by IIS signalling in the ASI neurons⁵² and so therefore it is possible that neuronal SKN-1B also has a role in regulating DAF-7/TGF- β to control longevity effects in the BD method.

4.2.2 DAF-16 localisation in response to DR is short-lived in *skn-1b* mutants

Our finding that the nuclear localisation and expression of DAF-16 in *Ex[pNL213(*ges-1p::GFP::daf-16*) + *rol-6(su1006)*]* worms co-expressing the $\Delta skn-1b$ mutation is short lived implicates behavioural changes that may be controlled by SKN-1B. It was shown that SKN-1B is not required for DAF-16 localisation and expression changes immediately induced by BD ($P < 0.0001$, $N \geq 59$; $P < 0.001$, $N \geq 53$) or by IDR ($P < 0.0001$, $N \geq 53$) as there was a significant increase in $\Delta skn-1b$ mutant worms (Figure 6). A modification of the BD protocol was made to include refeeding post-starvation to investigate the longer-term effects of DAF-16 localisation and expression, as it is known that DAF-16 levels remain high after refeeding to regulate a quiescent behavioural state.³⁷ After 6 hours of refeeding, DAF-16 localisation and expression were reduced almost to the level of the fed control in $\Delta skn-1b$ mutants ($P > 0.05$, $N \geq 53$; $P < 0.05$,

N \geq 53), whereas in N2 worms this was consistently elevated (P<0.0001, N=>59; P<0.0001, N \geq 59).

In N2 worms, starvation and refeeding is a method of inducing quiescent behaviour that is dependent on DAF-16. Elevated levels of DAF-16 are required for quiescent sleep-like behaviour under these conditions; and quiescence usually resolves within 24 hours post-refeeding.⁵³ This data suggests that $\Delta skn-1b$ worms are unable to appropriately maintain DAF-16 levels in the intestine following refeeding after starvation, which may correlate with a behavioural defect such as reduced quiescence; though this is yet to be shown. The reduced ability for $\Delta skn-1b$ mutants to maintain DAF-16 nuclear localisation in the intestine could also be related to DAF-7/TGF- β signalling as previously mentioned, as DAF-7/TGF- β is also required for this effect and exclusively expressed in the ASI neurons.²⁷ Interactions between SKN-1B and DAF-7/TGF- β remain to be investigated.

4.2.3 Expression of *sod-3::GFP* is SKN-1B dependent in IDR

We next asked whether the DAF-16 localisation and expression observed is related to its transcriptional activity in the downstream DAF-16-specific gene *sod-3*. For this, we used *wuEx43[pPD95.77 sod-3::GFP, rol-6(su1006)]* worms. We observed no significant change to *sod-3::GFP* expression between N2 and $\Delta skn-1b$ worms in fed (P>0.05, N \geq 57) or fasted (P>0.05, N \geq 59) conditions using the BD protocol, suggesting that intestinal DAF-16 activity is unchanged in $\Delta skn-1b$ mutant worms.

Interestingly though, there was a significant reduction in *sod-3::GFP* expression in fasted conditions in $\Delta skn-1b$ worms using the IDR protocol (P<0.0001, N \geq 57). The level of *sod-3::GFP* induction using IDR was also much lower (maximum ~1.3-fold) compared to BD (maximum ~2-fold), which exemplifies the complex nature of DR pathways in *C. elegans*. This difference may be the effect of sensory perception of food in liquid media, as this is known to interfere with IIS signalling in an undefined way.³⁷

As the IDR method extends lifespan in a SKN-1B-dependent fashion, it is interesting how the same method demonstrates an overall reduced expression of this DAF-16 target gene and no change to *sod-3* expression under DR conditions in $\Delta skn-1b$ worms. As *sod-3* is a mitochondrial oxidative stress response gene, this may indicate a lower level of stress experienced by worms in IDR than BD. Additionally, as it was shown that SKN-1B is not required for the expression of *sod-3* in BD, the difference in expression in IDR conditions must be due to another unknown factor or role of SKN-1B. This phenotype may further suggest either that $\Delta skn-1b$ worms are unable to appropriately respond to oxidative stress, or that they are more capable of reducing stress levels in certain environmental contexts, indicated by the low expression of *sod-3*, however this is unclear.

4.3 SKN-1B and the UPR_{ER}

4.3.1 Expression, but not induction, of *hsp-4* is regulated by SKN-1B

As SKN-1 is known to transcriptionally regulate many of the UPR_{ER} components, it was hypothesised that SKN-1B could be required for distal tissues to appropriately express UPR_{ER} genes. In *zcls4[hsp-4::GFP]* V worms, it was found that $\Delta skn-1b$ worms had a significantly lower expression of *hsp-4::GFP* under fed conditions ($P < 0.0001$, $N \geq 62$), suggesting that SKN-1B may indirectly positively regulate *hsp-4* and therefore the UPR_{ER} in tissues outside the ASI neurons. Starvation by BD had the effect of significantly reducing the expression of *hsp-4::GFP* in both N2 ($P < 0.0001$, $N \geq 62$) and further in $\Delta skn-1b$ worms ($P < 0.0001$, $N \geq 65$) contrary to the notion that DR induces expression of UPR_{ER} components and extends lifespan through IRE-1 dependent pathways.⁵⁴ This difference may be due to the BD method which could reduce global translation and therefore ER folding workload due to nutrient limitation.

To induce the UPR_{ER} there are multiple methods. Here, we employed *ero-1* RNAi, as chemical methods such as tunicamycin may have off-target effects which are difficult to distinguish. Ero-1 is an oxidoreductase that effectively reoxidises the PDI-1 protein disulphide isomerase which is a crucial step in the ERAD. By preventing this stage of the ERAD, misfolded proteins

accumulate in the ER lumen and activate the UPR_{ER}, which is shown by a large 6-fold increase in *hsp-4::GFP* expression in both N2 ($P < 0.0001$, $N \geq 54$) and $\Delta skn-1b$ ($P < 0.0001$, $N \geq 56$) worms. Although *hsp-4::GFP* expression is basally lower in $\Delta skn-1b$ worms, the induction of the UPR_{ER} by *ero-1* RNAi seems to be independent of SKN-1B ($P > 0.05$, $N \geq 54$), suggesting that the role of SKN-1B here may only be to transcriptionally regulate UPR_{ER} components in non-stressed conditions.

4.3.2 Ero-1 extends lifespan independently of SKN-1B

It has been previously characterised that *ero-1* RNAi extends lifespan through initiation of the UPR_{ER} and primarily exerts this phenotype through IRE-1-dependent signalling. Therefore, it was next investigated whether SKN-1B is required for the longevity effects of the UPR_{ER} by *ero-1* RNAi and whether this affected SKN-1B expression itself.

It was first found that *ero-1* RNAi moderately induced the expression of *skn-1b* in *wuEx217[skn-1b::GFP::skn-1 3'UTR]* worms to a significant level ($P < 0.05$, $N \geq 55$). This has been shown to be independent of the action of the UPR_{ER} in whole worm fluorescence, and so therefore may be more indicative of SKN-1B activity to restore protein homeostasis within the ASI neurons.

Lifespan analysis of N2 and $\Delta skn-1b$ worms revealed that whereas *ero-1* RNAi successfully extended N2 lifespan by $>50\%$ ($P < 0.0001$, $N \geq 180$) it also did so in $\Delta skn-1b$ mutants ($P < 0.0001$, $N \geq 180$) without any significant difference between these two genotypes ($P > 0.05$, $N \geq 180$). This data shows that whereas SKN-1B may have a role in transcriptional regulation of UPR_{ER} components, and is itself upregulated by ER stress, it does not have any role in the determination of lifespan by *ero-1* RNAi.

4.4 SKN-1B and the mitochondria

4.4.1 $\Delta skn-1b$ mutants have an associated mitochondrial morphology defect

To assess whether changes in signalling by $\Delta skn-1b$ mutation contribute to any physiological differences, the mitochondrial network morphology within the body wall muscle of *wbmEx289[myo-3p::tomm20(aa1-49)::GFP::unc54 3'UTR]* worms was investigated. This also included BD DR conditions as it is known that starvation contributes to a disorganised mitochondrial network morphology associated with mitophagy due to energy imbalance.

For this, average coverage of mitochondria in whole fibres as well as average area of individual mitochondria within fibres were measured. Here, we found a significant decrease in the area coverage and mitochondrial size in $\Delta skn-1b$ worms compared to N2 in both fed ($P < 0.0001$, $N \geq 54$; $P < 0.0001$, $N \geq 518$) and starved ($P < 0.001$, $N \geq 49$; $P < 0.001$, $N \geq 518$) conditions. Starvation also had the effect of reducing both coverage and area in N2 ($P < 0.0001$, $N \geq 49$; $P < 0.0001$, $N \geq 518$) and $\Delta skn-1b$ ($P < 0.0001$, $N \geq 57$; $P < 0.0001$, $N \geq 518$) worms independently as expected. Fed $\Delta skn-1b$ worms showed a modest but significant decrease in average area, as the networks seen were not so sparsely distributed but exhibited a much greater degree of fragmentation, and therefore decrease in average mitochondrial area. This data suggests that SKN-1B is required for normal mitochondrial network morphology, and it is still able to adapt to changes. If SKN-1B was causing a defect in the dynamic remodelling of mitochondrial networks, the phenotype may be more severe than the one observed; but as SKN-1 is involved in regulating mitophagy, this may also include SKN-1B to an extent in order to cause a minor phenotypic change that doesn't affect physiology or lifespan.

The morphology changes seen here may also be in-part explained by the difference in *sod-3* expression by specific IDR starvation. If $\Delta skn-1b$ mutant worms, in certain contexts, are unable to respond adequately to oxidative stress by under-expression of mitochondrial *sod-3*, then this could result in damage to organelles and an increased rate of mitophagy. This is supported by the fact that high SOD-3 levels are associated with superior mitochondrial health and

longevity phenotypes.⁵⁵ On the other hand, in this study it was shown that there is no difference in *sod-3* expression between N2 and Δ *skn-1b* in fed conditions, though there is a difference in mitochondrial morphology; meaning that if SOD-3 is linked at all to this phenotype it is a combinatory effect with other factors.

References

1. Rupert PB, Daughdrill GW, Bowerman B, Matthews BW. A new DNA-binding motif in the Skn-1 binding domain-DNA complex. *Nat Struct Biol.* 1998. doi:10.1038/nsb0698-484.
2. Zhang Y, Crouch DH, Yamamoto M, Hayes JD. Negative regulation of the Nrf1 transcription factor by its N-terminal domain is independent of Keap1: Nrf1, but not Nrf2, is targeted to the endoplasmic reticulum. *Biochem J.* 2006. doi:10.1042/bj20060725.
3. Wen H, Yang H, An YJ, et al. Enhanced Phase II Detoxification Contributes to Beneficial Effects of Dietary Restriction as Revealed by Multi-platform Metabolomics Studies. *Mol Cell Proteomics.* 2013. doi:10.1074/mcp.m112.021352.
4. An JH, Blackwell TK. SKN-1 links *C. elegans* mesendodermal specification to a conserved oxidative stress response. *Genes Dev.* 2003. doi:10.1101/gad.1107803.
5. Tullet JMA, Hertweck M, An JH, et al. Direct Inhibition of the Longevity-Promoting Factor SKN-1 by Insulin-like Signaling in *C. elegans*. *Cell.* 2008. doi:10.1016/j.cell.2008.01.030.
6. Inoue H, Hisamoto N, Jae HA, et al. The *C. elegans* p38 MAPK pathway regulates nuclear localization of the transcription factor SKN-1 in oxidative stress response. *Genes Dev.* 2005. doi:10.1101/gad.1324805.
7. Bishop NA, Guarente L. Two neurons mediate diet-restriction-induced longevity in *C. elegans*. *Nature.* 2007. doi:10.1038/nature05904.
8. Satoh T, Okamoto S -i., Cui J, et al. Activation of the Keap1/Nrf2 pathway for neuroprotection by electrophilic phase II inducers. *Proc Natl Acad Sci.* 2006. doi:10.1073/pnas.0505723102.
9. Chen P-C, Vargas MR, Pani AK, et al. Nrf2-mediated neuroprotection in the MPTP mouse model of Parkinson's disease: Critical role for the astrocyte. *Proc Natl Acad Sci.* 2009. doi:10.1073/pnas.0813361106.
10. Stack C, Ho D, Wille E, et al. Triterpenoids CDDO-ethyl amide and CDDO-trifluoroethyl amide improve the behavioral phenotype and brain pathology in a transgenic mouse model of Huntington's disease. *Free Radic Biol Med.* 2010. doi:10.1016/j.freeradbiomed.2010.03.017.
11. Anderson JL, Morran LT, Phillips PC. Outcrossing and the maintenance of males

- within *C. elegans* populations. In: *Journal of Heredity*. ; 2010.
doi:10.1093/jhered/esq003.
12. Sulston JE, Horvitz HR. Post-embryonic cell lineages of the nematode, *Caenorhabditis elegans*. *Dev Biol*. 1977. doi:0012-1606(77)90158-0 [pii].
 13. Kimble J, Hirsh D. The postembryonic cell lineages of the hermaphrodite and male gonads in *Caenorhabditis elegans*. *Dev Biol*. 1979. doi:10.1016/0012-1606(79)90035-6.
 14. Sulston JE, Schierenberg E, White JG, Thomson JN. The embryonic cell lineage of the nematode *Caenorhabditis elegans*. *Dev Biol*. 1983. doi:10.1016/0012-1606(83)90201-4.
 15. Hillier LDW, Coulson A, Murray JI, Bao Z, Sulston JE, Waterston RH. Genomics in *C. elegans*: So many genes, such a little worm. *Genome Res*. 2005. doi:10.1101/gr.3729105.
 16. Lai CH, Chou CY, Ch'ang LY, Liu CS, Lin WC. Identification of novel human genes evolutionarily conserved in *Caenorhabditis elegans* by comparative proteomics. *Genome Res*. 2000. doi:10.1101/gr.10.5.703.
 17. Conte D, MacNei LT, Walhout AJM, Mello CC. RNA Interference in *Caenorhabditis elegans*. *Curr Protoc Mol Biol*. 2015. doi:10.1002/0471142727.mb2603s109.
 18. Murphy CT, Hu PJ. Insulin/insulin-like growth factor signaling in *C. elegans*. *WormBook*. 2013. doi:10.1895/wormbook.1.164.1.
 19. An JH, Vranas K, Lucke M, et al. Regulation of the *Caenorhabditis elegans* oxidative stress defense protein SKN-1 by glycogen synthase kinase-3. *Proc Natl Acad Sci*. 2005. doi:10.1073/pnas.0508105102.
 20. Zheng S, Chiu H, Boudreau J, Papanicolaou T, Bendena W, Chin-Sang I. A functional study of all 40 *C. elegans* insulin-like peptides. *J Biol Chem*. September 2018:jbc.RA118.004542. doi:10.1074/jbc.RA118.004542.
 21. Murphy CT, Lee S-J, Kenyon C. Tissue entrainment by feedback regulation of insulin gene expression in the endoderm of *Caenorhabditis elegans*. *Proc Natl Acad Sci U S A*. 2007;104(48):19046-19050. DOI: 10.1073/pnas.0709613104. doi:10.1073/pnas.0709613104.
 22. Dorman JB, Albinder B, Shroyer T, Kenyon C. The *age-1* and *daf-2* genes function in a common pathway to control the lifespan of *Caenorhabditis elegans*. *Genetics*. 1995.

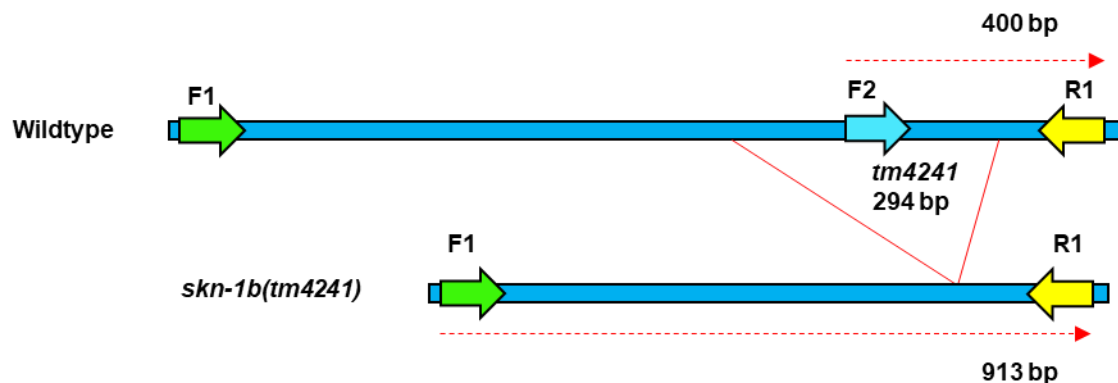
23. Apfeld J, Kenyon C. Regulation of lifespan by sensory perception in *Caenorhabditis elegans*. *Nature*. 1999. doi:10.1038/45544.
24. Artan M, Jeong DE, Lee D, et al. Food-derived sensory cues modulate longevity via distinct neuroendocrine insulin-like peptides. *Genes Dev*. 2016. doi:10.1101/gad.279448.116.
25. Li C, Kim K. Neuropeptides. *WormBook*. 2008;(212):1-36. doi:10.1895/wormbook.1.142.1.
26. Hung WL, Wang Y, Chitturi J, Zhen M. A *Caenorhabditis elegans* developmental decision requires insulin signaling-mediated neuron-intestine communication. *Development*. 2014. doi:10.1242/dev.103846.
27. Fletcher M, Kim DH. Age-Dependent Neuroendocrine Signaling from Sensory Neurons Modulates the Effect of Dietary Restriction on Longevity of *Caenorhabditis elegans*. *PLoS Genet*. 2017. doi:10.1371/journal.pgen.1006544.
28. Katewa SD, Kapahi P. Dietary restriction and aging, 2009. *Aging Cell*. 2010. doi:10.1111/j.1474-9726.2010.00552.x.
29. Lakowski B, Hekimi S. The genetics of caloric restriction in *Caenorhabditis elegans*. *Proc Natl Acad Sci*. 1998. doi:10.1073/pnas.95.22.13091.
30. Houthoofd K, Braeckman BP, Lenaerts I, et al. No reduction of metabolic rate in food restricted *Caenorhabditis elegans*. *Exp Gerontol*. 2003. doi:10.1016/s0531-5565(02)00172-9.
31. Gruber J, Soon YT, Halliwell B. Evidence for a trade-off between survival and fitness caused by resveratrol treatment of *Caenorhabditis elegans*. In: *Annals of the New York Academy of Sciences*. ; 2007. doi:10.1196/annals.1395.059.
32. Szewczyk NJ, Udranszky IA, Kozak E, et al. Delayed development and lifespan extension as features of metabolic lifestyle alteration in *C. elegans* under dietary restriction. *J Exp Biol*. 2006. doi:10.1242/jeb.02492.
33. Hosono R, Nishimoto S, Kuno S. Alterations of life span in the nematode *Caenorhabditis elegans* under monoxenic culture conditions. *Exp Gerontol*. 1989. doi:10.1016/0531-5565(89)90016-8.
34. Kaeberlein TL, Smith ED, Tsuchiya M, et al. Lifespan extension in *Caenorhabditis elegans* by complete removal of food. *Aging Cell*. 2006. doi:10.1111/j.1474-9726.2006.00238.x.

35. Panowski SH, Wolff S, Aguilaniu H, Durieux J, Dillin A. PHA-4/Foxa mediates diet-restriction-induced longevity of *C. elegans*. *Nature*. 2007. doi:10.1038/nature05837.
36. Greer EL, Dowlatshahi D, Banko MR, et al. An AMPK-FOXO Pathway Mediates Longevity Induced by a Novel Method of Dietary Restriction in *C. elegans*. *Curr Biol*. 2007;17(19):1646-1656. doi:10.1016/j.cub.2007.08.047.
37. McCloskey RJ, Fouad AD, Churgin MA, Fang-Yen C. Food responsiveness regulates episodic behavioral states in *Caenorhabditis elegans*. *J Neurophysiol*. 2017. doi:10.1152/jn.00555.2016.
38. Labbadia J, Morimoto RI. The Biology of Proteostasis in Aging and Disease. *Annu Rev Biochem*. 2015. doi:10.1146/annurev-biochem-060614-033955.
39. Rubio C, Pincus D, Korennykh A, Schuck S, El-Samad H, Walter P. Homeostatic adaptation to endoplasmic reticulum stress depends on Ire1 kinase activity. *J Cell Biol*. 2011. doi:10.1083/jcb.201007077.
40. Taylor RC, Dillin A. XXBP-1 Is a cell-nonautonomous regulator of stress resistance and longevity. *Cell*. 2013. doi:10.1016/j.cell.2013.05.042.
41. Harding HP, Zhang Y, Bertolotti A, Zeng H, Ron D. Perk is essential for translational regulation and cell survival during the unfolded protein response. *Mol Cell*. 2000. doi:10.1016/S1097-2765(00)80330-5.
42. Shen X, Ellis RE, Sakaki K, Kaiserman RJ. Genetic interactions due to constitutive inducible gene regulation mediated by the unfolded protein in *C. elegans*. *PLoS Genet*. 2005. doi:10.1371/journal.pgen.0010037.
43. Li X, Matilainen O, Jin C, Glover-Cutter KM, Holmberg CI, Blackwell TK. Specific SKN-1/Nrf stress responses to perturbations in translation elongation and proteasome activity. Kim SK, ed. *PLoS Genet*. 2011;7(6):e1002119. doi:10.1371/journal.pgen.1002119.
44. Glover-Cutter KM, Lin S, Blackwell TK. Integration of the Unfolded Protein and Oxidative Stress Responses through SKN-1/Nrf. Garsin DA, ed. *PLoS Genet*. 2013;9(9):e1003701. doi:10.1371/journal.pgen.1003701.
45. Oliveira RP, Abate JP, Dilks K, et al. Condition-adapted stress and longevity gene regulation by *Caenorhabditis elegans* SKN-1/Nrf. *Aging Cell*. 2009;8(5):524-541. doi:10.1111/j.1474-9726.2009.00501.x.
46. Barja G. The mitochondrial free radical theory of aging. *Prog Mol Biol Transl Sci*.

- 2014;127:1-27. doi:10.1016/B978-0-12-394625-6.00001-5.
47. Weir HJ, Yao P, Huynh FK, et al. Dietary Restriction and AMPK Increase Lifespan via Mitochondrial Network and Peroxisome Remodeling. *Cell Metab.* 2017;26(6):884-896.e5. doi:10.1016/j.cmet.2017.09.024.
 48. Herzig S, Shaw RJ. AMPK: Guardian of metabolism and mitochondrial homeostasis. *Nat Rev Mol Cell Biol.* 2018;19(2):121-135. doi:10.1038/nrm.2017.95.
 49. Palikaras K, Lionaki E, Tavernarakis N. Coordination of mitophagy and mitochondrial biogenesis during ageing in *C. elegans*. *Nature.* 2015;521(7553):525-528. doi:10.1038/nature14300.
 50. Paek J, Lo JY, Narasimhan SD, et al. Mitochondrial SKN-1/Nrf mediates a conserved starvation response. *Cell Metab.* 2012;16(4):526-537. doi:10.1016/j.cmet.2012.09.007.
 51. Shaham S, ed. Methods in Cell Biology. In: *WormBook, Ed. The C. Elegans Research Community, WormBook.* ; 2006. doi:doi/10.1895/wormbook.1.49.1.
 52. Bargmann CI, Horvitz HR. Control of larval development by chemosensory neurons in *Caenorhabditis elegans*. *Science (80-).* 1991. doi:10.1126/science.2006412.
 53. Driver RJ, Lamb AL, Wyner AJ, Raizen DM. DAF-16/FOXO regulates homeostasis of essential sleep-like behavior during larval transitions in *C. elegans*. *Curr Biol.* 2013. doi:10.1016/j.cub.2013.02.009.
 54. Matai L, Sarkar GC, Chamoli M, et al. Dietary restriction improves proteostasis and increases life span through endoplasmic reticulum hormesis. *Proc Natl Acad Sci.* August 2019:201900055. doi:10.1073/PNAS.1900055116.
 55. Senchuk MM, Dues DJ, Schaar CE, et al. Activation of DAF-16/FOXO by reactive oxygen species contributes to longevity in long-lived mitochondrial mutants in *Caenorhabditis elegans*. *PLoS Genet.* 2018. doi:10.1371/journal.pgen.1007268

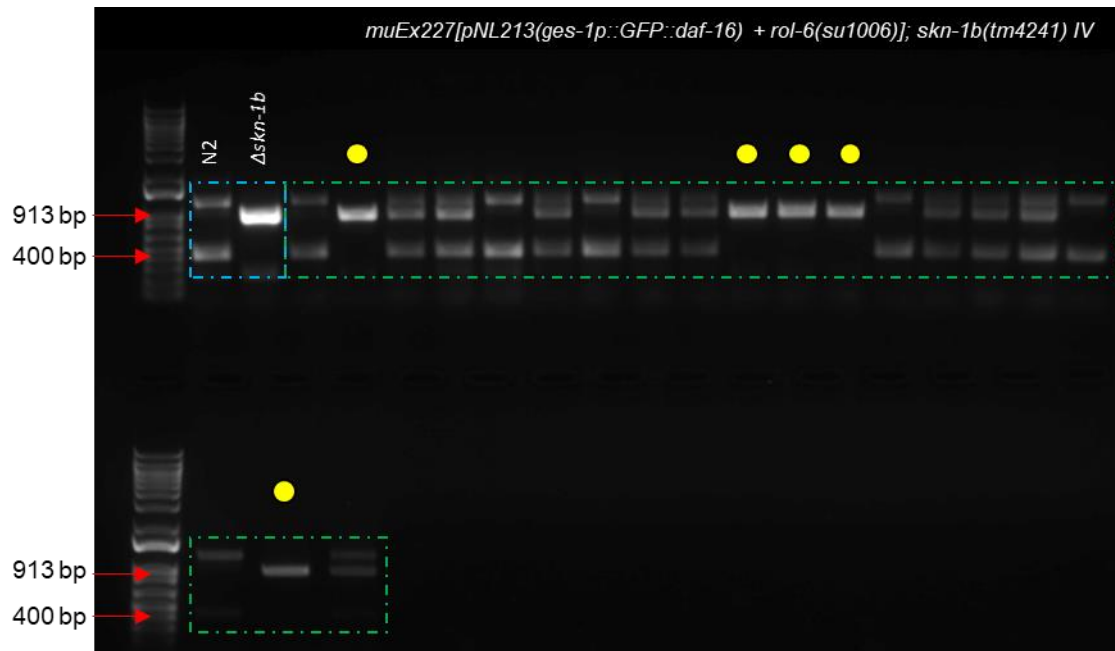
Supplementary information

```
//gctgattgaatggaaaacaatcatagagatgatgggtgtcaaatttctcagcaaataaattttaacaatttc
tatcatttcagccactcactgccgaagagaatgctcgatatgaagatctttcgaaaggattctataatggattc
ttcgagtcgttcaataacaatcaatatcagcagaaacatcagcaacaacaacgagaacaaataaagacacc
aactcttgaacatccaactcaaaaagccgaattggaagatgatctgtttgatgaagatcttgctcagcttttcg
aggatgtttcaagagaagaaggacaattgaatcaacttttgataataagcaacaacatccagttatcaata
atgtttctctgtcggagggaattgtttataatcaggcaaattgatggtttgatttaattattgtgtttcattca
acattttttattttcagtgaccgagatgcaagagatgctgatttctgcaatcaagtttccatttcaacaattcc
aacaacatcgactgctcaaccagagactttgttcaatgtaaccgattcacagactgtcgaacagtggcttcca
acagaagttgtaccaaacgatggtgagttgctgctggttgcactttctctctttttctctcccgtctattctcg
ctatctctatctattctttatcaattcgtgtgctctaatttttctgacaaaagttgagagactaatgaagg
aggcgtgccattgttgaacttctgaaatgaaagcgtagtttggtgggcggagcctcaatctggagccttatcct
cctttatttgctctcttataaacgactgaaattcaaactcccaccgaaatgtcacttccatctgattttgctcctc
tcttctggcatcctctaccaccaccaacaccaccaacaccgctccagcagctgtcaactctttgacgaacaa
gaagaagaatccaagaagatactgaacatgtaccttcaaattgtcaatcaacaacaggtggatcaacacgg
ccatcatcaccaacatccatacgcctattcaggagctcgcagcacttttgacagaggttctatctctctctct
ctctctctctttcatcctatctagacattccaacatttctcctttcagggtccctcatatcttggaaatggcag
agggttgtaacctaga//
```



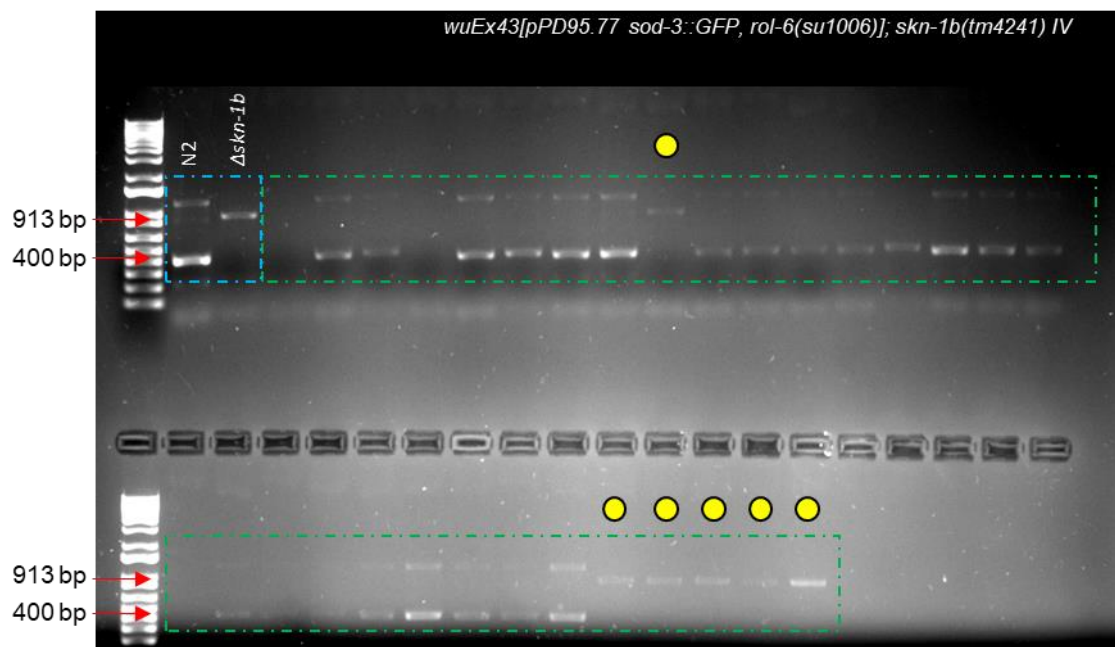
Supplementary Figure 1 – PCR primer strategy for *skn-1b(tm4241)* genotyping

A three-primer strategy including an internal primer annealing site (light blue) within the *tm4241* deletion (pink). Forward and reverse primer annealing sites shown in green and yellow respectively. Flanking regions of *tm4241* deletion are shown in grey. Below, expected band sizes of wildtype and *skn-1b(tm4241)* alleles are shown.



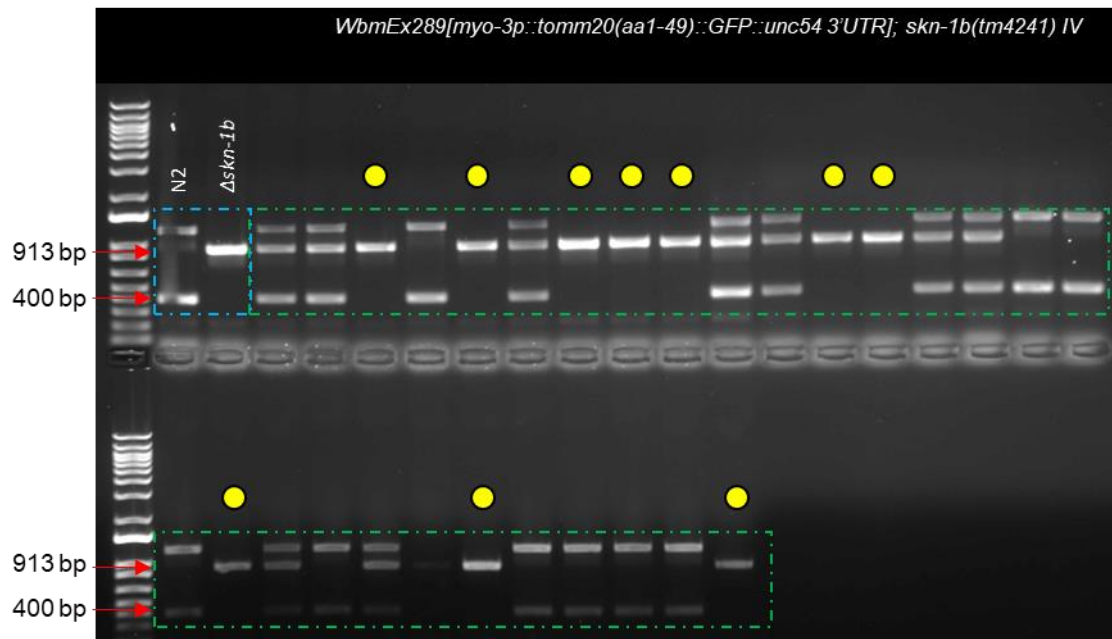
Supplementary Figure 2 – Validation of *daf-16::GFP;skn-1b(tm4241)* cross using single-worm PCR

Lanes represent PCR products from individual worms that were allowed to generate clonal offspring prior to lysis. N2 and *skn-1b(tm4241)* worms used as a control in the first two wells (blue rectangle) showing homozygosity for expected 400bp (wildtype allele) and 913bp (*tm4241* deletion). The green rectangle represents all other samples. Yellow circles above lanes indicate homozygous *skn-1b(tm4241)* mutants.



Supplementary Figure 3 – Validation of *sod-3::GFP;skn-1b(tm4241)* cross using single-worm PCR

Each lane represents PCR product derived from single worm lysis post egg-laying. N2 and *skn-1b(tm4241)* controls are shown in a blue rectangle and demonstrate homozygosity for wildtype and *tm4241* deletion alleles respectively, all other samples are in a green rectangle. Yellow circles above lanes indicate homozygous *skn-1b(tm4241)* mutants.



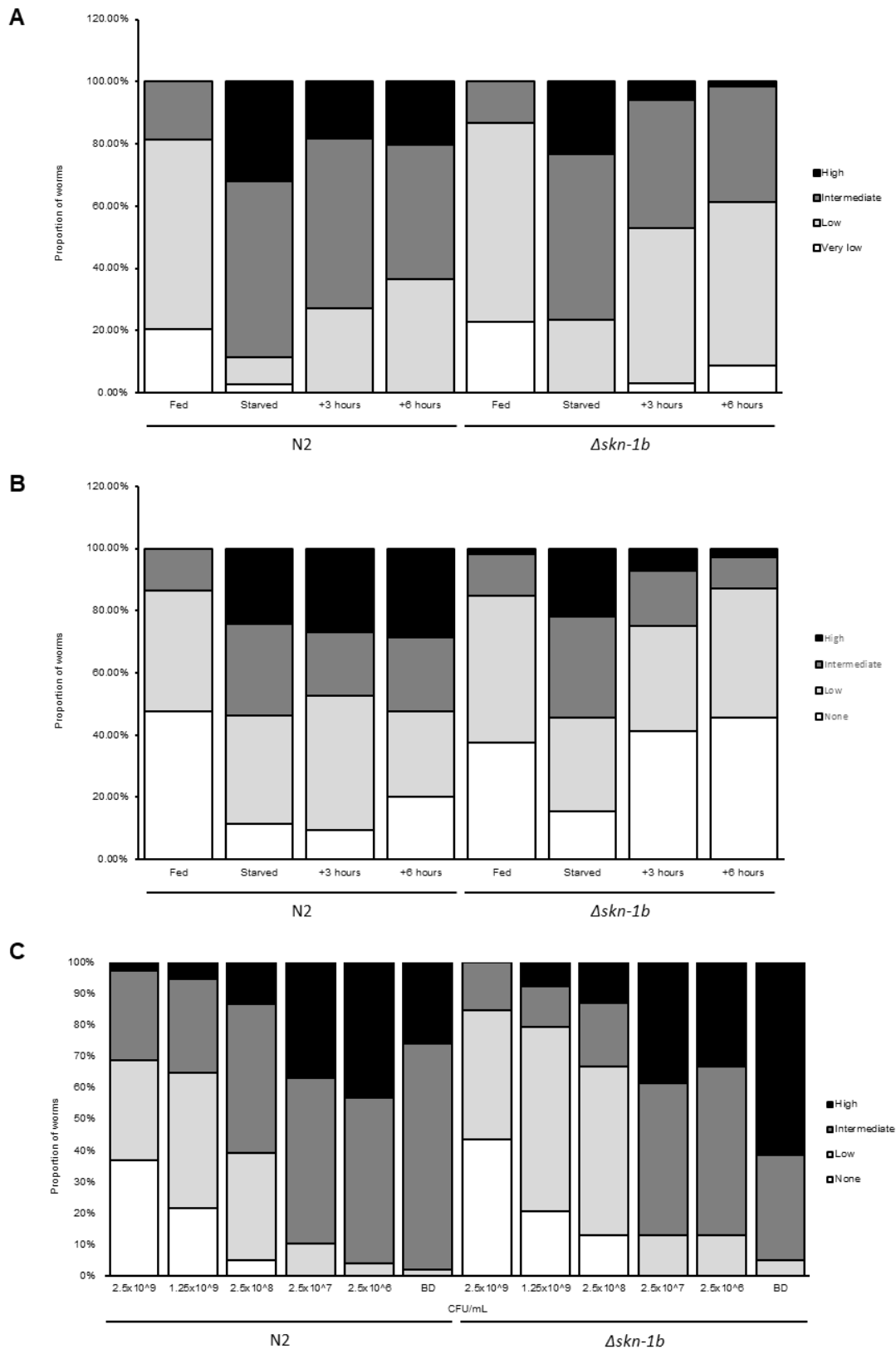
Supplementary Figure 4 – Validation of *tomm20::GFP;skn-1b(tm4241)* cross using single-worm PCR

Lanes represent PCR products from single worms after being allowed to generate offspring. N2 and *skn-1b(tm4241)* controls are shown in a blue rectangle with homozygosity for wildtype and *tm4241* deletion alleles respectively, all other samples are shown in a green rectangle. Yellow circles represent homozygous *skn-1b(tm4241)* mutants.

Trial 1		Trial 2		Trial 3		Trial 4		Trial 5	
N2 fed	N2 starved	N2 fed	N2 starved	N2 fed	N2 starved	N2 fed	N2 starved	N2 fed	N2 starved
1.271542604	1.369362553	0.4650793	1.548352182	1.534897258	0.873573229	0.740402404	1.033523989	0.846244177	0.872785779
0.93887164	0.711790531	1.262592761	2.199143591	1.456779846	1.340763161	0.331041471	1.645424305	0.879196004	0.99524469
1.356447826	1.115760128	0.941198567	1.831908704	1.290233439	1.622899328	0.92909804	0.674568431	1.322042701	0.77317124
0.977134652	0.956264954	1.871223465	1.632699058	1.147377915	1.473659737	0.477545296	1.995617105	0.325207258	0.871307613
0.940047518	0.724867546	0.451549929	1.268029976	1.185475297	1.860333154	1.113972371	1.471508221	0.766372406	2.015465652
1.112770608	0.662170189	0.376543094	1.520204723	0.994426749	1.405923244	0.732473037	0.971771195	0.760336261	1.932648446
0.954869844	1.457177574	1.141707033	1.620252036	1.293117908	1.149693811	0.946996083	0.53763131	0.867312572	2.440919392
0.845348059	1.757900532	0.989375862	1.359838698	1.075865462	0.908497892	1.098016344	0.713421562	0.810760946	1.486191685
1.054406632	1.678578595	0.63125818	0.994284636	0.754549247	1.28288656	0.67887748	1.192078044	0.873926181	0.921162097
1.003801172	1.551486973	1.041233146	1.39789284	0.1976228	2.048175305	1.3407812	1.382777145	1.264742913	0.890974112
1.22583711	1.547768579	0.538144272	0.412871844	0.712039974	1.172237643	0.817147258	1.052455128	0.975327593	1.478223393
0.707770338	1.092168543	0.645647064	0.617060298	0.611914615	1.483202655	1.147917333	1.122618633	1.086404269	0.919894579
0.824190797	1.262371895	0.489865108	0.890194429	1.460990656	0.565610561	0.900404331	1.721095097	1.22645589	1.889298616
0.324419888	1.599700816	1.168434703	1.565816213	0.564405067	2.329046545	1.091187923	1.820017599	1.923118457	1.931079484
0.695769549	1.362777067	1.63371774	1.433489412	0.758844253	1.343798193	1.389620928	2.073164625	1.47322596	1.403189254
1.53442393	0.852346383	1.405730325	1.081528389	0.836056307	1.569789234	1.118676992	1.225950037	0.645402555	1.402724376
2.057137271	0.935987465	1.722203011	0.808674396	1.284057386		1.232923118	1.1047974	1.056949919	1.880712909
0.489168077	1.359525608	1.042926705	1.141490563	0.841345822		1.066428173	0.92818912	0.737753382	0.95502552
0.976980905	1.725522605	0.284441502	1.290803887			0.592298368	1.0535996	0.92339932	1.523145817
0.979782513	1.916273925	0.224224658	1.093873543			0.740256465	2.044477317	0.877913959	1.363445856
1.114100233	1.90959733	1.205088158	0.942713857			0.633848815	2.835786923	0.584939421	1.333199762
1.239640152	1.398264096	1.801240007	1.220521191			1.168663753	1.543375631	1.447189186	3.019419533
0.964991505	1.211208391	1.017045814	1.486550014			0.646875815	1.113893001	0.63591978	2.127072579
0.355644715	1.188263112	0.821611658	1.536656439			0.396243041	1.373543286	1.68985889	1.390546764
0.448214497		0.767347738	0.599538967			1.312099012	1.305531745		1.724198086
1.167202654		0.852464992	0.513186561			1.084217402	1.120263122		1.145545408
1.439485309		1.443618932	1.519867285			0.466690743	1.724026684		2.458533892
		1.29050465	1.993611749			1.057854881	1.836449849		
		0.79413271	2.295568216			1.46006607	2.414037795		
		0.840508211	2.153895007			1.00680302	1.911326936		
		1.313991638	1.359202022			0.927598962	1.150484072		
		1.525349068	1.513296785			1.311213135	1.826454289		
						1.41023165	2.609380068		
						2.147936738	2.715390866		
						1.040282001	1.213664255		
						1.421086203	0.955103394		
						0.994806556			
						1.027417582			

Supplementary Figure 5 – Raw data for bacterial deprivation (BD) *skn-1b::GFP* fluorescence

Numbers represent fold-change in *skn-1b::GFP* fluorescence intensity measured using ImageJ. A Student's T-test was used to determine statistical significance between N2 starved and N2 fed worms with pooled data. Data obtained from Dr. Max Thompson.



Supplementary Figure 7 – Proportions of worms graded in *daf-16::GFP* experiments

(A) Percentage of worms graded “None”, “Low”, “Intermediate” or “High” for nuclear *daf-16::GFP* in fed, starved and 3/6 hours post-refeeding. (B) Percentage of worms graded “Very Low”, “Low”, “Intermediate” or “High” for *daf-16::GFP* expression levels in fed, starved and 3/6 hours post-refeeding. (C) Percentage of worms graded “None”, “Low”, “Intermediate” or “High” for nuclear *daf-16::GFP* after 16 hours IDR at different bacterial dilutions.

Trial 1										Trial 2														
N2					Δskn-1b					N2					Δskn-1b									
2.5x10 ⁹	1.25x10 ⁹	2.5x10 ⁸	2.5x10 ⁷	2.5x10 ⁶	BD	2.5x10 ⁹	1.25x10 ⁹	2.5x10 ⁸	2.5x10 ⁷	2.5x10 ⁶	BD	2.5x10 ⁹	1.25x10 ⁹	2.5x10 ⁸	2.5x10 ⁷	2.5x10 ⁶	BD	2.5x10 ⁹	1.25x10 ⁹	2.5x10 ⁸	2.5x10 ⁷	2.5x10 ⁶	BD	
1	2	3	3	3	3	0	0	0	3	3	3	2	1	2	2	2	3	2	1	2	1	3	1	1
0	0	2	3	2	3	1	0	2	3	3	3	1	2	2	2	3	3	2	1	2	2	2	3	2
0	1	3	2	3	2	1	0	1	2	3	3	2	1	2	2	2	2	1	1	1	2	2	2	2
0	1	2	3	3	1	0	1	3	3	2	2	1	1	2	3	3	2	0	1	0	2	2	2	3
1	2	0	3	2	2	0	1	1	2	3	2	1	0	2	2	2	2	1	2	2	1	2	2	2
2	0	2	3	1	2	0	2	1	2	2	3	2	1	2	2	3	3	2	1	3	2	1	1	1
1	1	2	2	1	2	0	1	0	2	2	3	1	2	3	2	2	2	1	0	1	3	3	2	2
2	2	1	2	2	3	0	0	1	2	2	2	0	1	1	3	2	2	1	3	1	2	3	3	3
2	3	2	1	2	3	0	0	1	2	2	2	2	1	1	2	2	2	0	1	1	3	2	2	2
1	2	1	2	2	3	1	3	1	2	2	3	2	1	1	2	2	3	2	2	1	3	2	2	2
0	0	0	3	3	2	0	3	0	2	2	3	1	2	1	3	2	2	2	1	1	2	2	3	3
0	1	1	1	2	2	1	1	2	3	1	3	1	1	1	3	3	2	1	0	3	2	3	2	2
0	0	2	3	2	2	2	1	0	3	1	3	0	2	1	2	2	2	0	1	1	1	2	3	3
2	1	0	2	3	1	1	1	2	2	2	3	2	2	2	2	2	2	0	1	2	2	2	2	3
2	1	3	2	2	2	0	0	1	2	2	3	2	1	2	2	2	2	0	1	3	2	3	3	3
1	1	2	2	2	2	0	0	2	2	3	3	0	2	2	3	3	2	0	1	3	3	2	3	3
3	1	2	2	2	2	1	1	2	2	2	2	1	0	2	1	3	2	0	1	1	2	3	3	3
1	3	2	2	2	2	2	2	2	2	2	2	0	1	3	2	3	2	0	1	2	1	1	3	3
2	0	2	2	2	2	2	2	2	2	2	2	1	1	2	3	2	2	1	1	1	1	3	3	3
2	2	2	2	2	2	2	2	2	2	2	2	1	0	2	3	3	2	1	1	2	3	2	3	3

Trial 3											
N2					Δskn-1b						
2.5x10 ⁹	1.25x10 ⁹	2.5x10 ⁸	2.5x10 ⁷	2.5x10 ⁶	BD	2.5x10 ⁹	1.25x10 ⁹	2.5x10 ⁸	2.5x10 ⁷	2.5x10 ⁶	BD
0	1	1	2	2	3	1	0	1	2	3	3
0	2	1	3	2	2	1	1	1	3	3	2
0	0	2	2	3	2	1	1	1	3	2	2
0	3	1	1	2	3	1	2	1	3	2	3
1	1	1	2	2	3	1	1	2	3	2	2
1	0	2	3	3	3	1	1	1	1	2	2
2	2	2	2	3	2	1	3	2	2	2	2
2	2	3	3	3	3	1	0	2	1	2	3
0	1	1	1	3	3	0	2	3	2	2	3
0	2	3	2	3	3	1	2	1	2	2	3
0	3	2	2	2	2	1	0	2	3	3	2
1	3	2	2	2	3	1	1	3	2	2	3
0	0	1	3	3	3	2	0	3	2	2	2
0	2	3	3	3	3	1	0	1	2	2	2
2	3	1	2	2	3	0	2	1	3	3	3
0	1	1	3	3	3	2	1	1	1	2	2
1	1	1	2	2	2	2	1	1	1	2	2
0	0	3	3	3	2	1	0	2	3	3	3
0	2	2	2	2	3	2	1	2	2	3	3
2	2	1	1	1	2	0	0	1	3	2	3

Nuclear localisation grading:
0 = None
1 = Low
2 = Intermediate
3 = High

Supplementary Figure 9 – Raw data for *daf-16::GFP* nuclear localisation grading after 16 hours IDR

Numbers represent grading of nuclear localisation of *daf-16::GFP* following 16-hours incubation at different bacterial dilutions. P-values of all comparisons are shown in a grid calculated by Chi-squared testing for pooled data.

	Trial 1				Trial 2				Trial 3			
	Fed		Starved		Fed		Starved		Fed		Starved	
	N2	Δ skn-1b	N2	Δ skn-1b	N2	Δ skn-1b	N2	Δ skn-1b	N2	Δ skn-1b	N2	Δ skn-1b
0.98795	1.51825	3.18801	3.38057	1.08434	1.06668	1.89429	1.22697	0.90483	0.90127	1.53470	0.88794	
1.08506	1.20582	2.95547	3.13340	0.79982	1.03600	1.14213	1.49837	1.11174	0.90610	0.98405	1.23322	
0.97258	0.86664	2.89029	4.17666	0.76414	1.32953	2.69340	1.24220	0.97992	0.84797	1.10239	1.23351	
0.84195	0.74154	2.97967	2.13294	1.15135	1.76782	1.52226	1.74667	1.13930	0.92542	1.54548	1.23224	
1.00279	0.76346	2.04999	2.33001	1.05687	0.84099	1.39706	1.08369	1.15356	1.45811	1.42638	1.35143	
1.02169	0.73680	1.92959	4.51840	1.25015	1.14096	1.36895	1.91760	1.16172	1.06977	1.16457	1.33152	
1.40728	0.55267	3.41571	4.47195	0.90414	1.32174	1.96525	1.41280	1.09524	0.85302	1.74470	1.46021	
1.25627	1.23863	3.14560	2.92715	0.93238	1.02096	1.32342	1.99498	0.91623	1.02198	1.47139	1.36176	
0.60593	1.24136	2.23403	2.56669	0.69124	0.84373	2.32981	1.73769	1.16094	0.82718	1.22167	1.21343	
0.71547	0.82828	2.51717	2.29950	1.08845	1.08314	1.95614	1.37460	1.23647	1.46986	1.40644	1.37589	
1.48432	0.86607	1.82696	2.97209	1.13358	1.41884	1.48744	1.96775	0.93511	1.01076	1.73232	1.34967	
1.58306	0.90180	1.64503	4.09119	0.78926	1.01529	1.13842	1.66724	0.81658	0.77212	1.23005	1.30244	
1.10190	0.73117	2.30929	4.20000	0.55754	1.04471	1.68349	1.38175	0.73140	1.02504	1.96859	1.49018	
0.85631	0.93565	2.26453	2.00983	1.09905	1.11739	1.38145	1.35364	0.93708	1.26795	1.97175	1.39680	
1.33399	1.36960	2.25185	2.36032	1.03638	1.27580	1.21881	1.74952	1.05385	0.86823	1.63302	0.93025	
0.74053	0.86625	1.75048	2.13015	1.18106	0.87318	2.10405	1.54756	0.94202	1.05847	1.59818	1.14054	
0.71067	1.57457	2.12470	2.51182	1.38018	1.68138	1.61821	1.84897	1.05846	0.79945	1.25148	1.60569	
0.57059	0.97450	1.81990	2.37603	0.74245		2.91847		1.11149	1.00487	1.46983	1.67668	
0.72166	0.69064		2.36209	0.99288		1.28001		0.69869	0.21210	0.28886	1.49424	
	1.41885		3.56745	1.36474				0.85539	0.05144	0.07006	1.75216	
	0.83435										1.53852	
	0.90645										1.35040	
											0.20940	
Average	1.00000	0.98924	2.40546	3.02591	1.00000	1.16930	1.70648	1.57365	1.00000	0.91756	1.34080	1.30079
StD	0.30105	0.28946	0.55620	0.85915	0.22412	0.26750	0.51463	0.27958	0.15162	0.33284	0.47882	0.31378

Supplementary Figure 10 – Raw data of *sod-3::GFP* expression after 16 hours BD in N2 and Δ skn-1b worms

Numbers represent fold-change in *sod-3::GFP* fluorescence intensity after 16 hours of dietary restriction by BD. P-Values of all group comparisons calculated by Two-Way ANOVA testing.

Table 1									
	N2		IDR		N2		IDR		
	2.5xIDV	1.25xIDV	2.5xIDV	1.25xIDV	2.5xIDV	1.25xIDV	2.5xIDV	1.25xIDV	
0.61294	0.73380	1.20442	1.08868	1.62036	1.48770	1.04047	1.03034	0.81930	0.71886
1.85271	0.90001	1.43402	0.96689	1.07834	0.70386	0.71886	0.88838	0.67382	0.88838
0.89128	0.89118	0.86754	1.51038	0.72955	1.42943	1.89817	1.46689	1.64226	1.46689
1.07028	0.80218	0.87711	1.07028	1.07021	0.86505	1.08842	1.62233	1.02303	1.02303
0.93039	0.93039	0.93039	1.07028	1.07021	1.23286	0.82117	1.81072	1.43836	1.43836
0.62742	1.07028	1.04885	1.51038	0.91136	1.54212	0.81930	0.97804	0.81930	0.97804
0.81372	1.03001	0.88865	1.51038	1.08882	2.80336	1.79971	0.81930	1.20399	1.20399
0.84278	1.24936	1.06432	1.96933	1.08882	0.82549	1.39914	1.00752	0.63962	0.88103
0.79891	0.81280	0.94011	1.06670	1.03643	0.94882	1.15139	1.10654	1.20075	0.93842
0.94656	1.15110	0.84207	1.05465	1.25811	0.82029	0.80535	0.93134	1.20075	0.93134
0.84656	1.11361	0.84207	0.97936	2.20123	0.90311	0.93641	0.80659	0.62737	0.93641
1.05794	1.16164	1.17874	0.91441	1.05589	0.94882	0.91675	0.75374	0.91675	0.75374
1.07893	1.11281	1.51605	1.08670	1.97611	1.57367	0.89396	1.39708	1.39708	1.39708
0.91090	1.61020	0.73645	1.56119	1.05047	1.13207	0.98162	1.00417	0.88162	1.00417
1.10222	0.64849	0.90715	1.20184	1.82765	1.06521	0.97426	1.08611	1.20323	1.08611
1.12308	0.88796	0.90490	1.64385	1.03635	0.82794	1.17116	0.87731	0.54002	0.61079
1.41386	1.14723	2.25714	0.97061	2.07061	1.58424	1.23885	1.07795	1.07795	1.07795
0.88535	1.06172	1.08894	1.08894	0.97426	1.07795	1.07795	1.07795	0.97426	0.97426
1.26079	1.26079	1.26079	1.26079	1.26079	1.26079	1.26079	1.26079	1.26079	1.26079
Average	1.00100	0.95066	1.08906	1.21665	1.31240	1.29706	1.08951	1.04546	0.93225
SD	0.28148	0.24571	0.36713	0.34481	0.44132	0.556494	0.30703	0.29379	0.24493
Table 2									
	N2		IDR		N2		IDR		
	2.5xIDV	1.25xIDV	2.5xIDV	1.25xIDV	2.5xIDV	1.25xIDV	2.5xIDV	1.25xIDV	
0.61294	0.73380	1.20442	1.08868	1.62036	1.48770	1.04047	1.03034	0.81930	0.71886
1.85271	0.90001	1.43402	0.96689	1.07834	0.70386	0.71886	0.88838	0.67382	0.88838
0.89128	0.89118	0.86754	1.51038	0.72955	1.42943	1.89817	1.46689	1.64226	1.46689
1.07028	0.80218	0.87711	1.07028	1.07021	0.86505	1.08842	1.62233	1.02303	1.02303
0.93039	0.93039	0.93039	1.07028	1.07021	1.23286	0.82117	1.81072	1.43836	1.43836
0.62742	1.07028	1.04885	1.51038	0.91136	1.54212	0.81930	0.97804	0.81930	0.97804
0.81372	1.03001	0.88865	1.51038	1.08882	2.80336	1.79971	0.81930	1.20399	1.20399
0.84278	1.24936	1.06432	1.96933	1.08882	0.82549	1.39914	1.00752	0.63962	0.88103
0.79891	0.81280	0.94011	1.06670	1.03643	0.94882	1.15139	1.10654	1.20075	0.93842
0.94656	1.15110	0.84207	1.05465	1.25811	0.82029	0.80535	0.93134	1.20075	0.93134
0.84656	1.11361	0.84207	0.97936	2.20123	0.90311	0.93641	0.80659	0.62737	0.93641
1.05794	1.16164	1.17874	0.91441	1.05589	0.94882	0.91675	0.75374	0.91675	0.75374
1.07893	1.11281	1.51605	1.08670	1.97611	1.57367	0.89396	1.39708	1.39708	1.39708
0.91090	1.61020	0.73645	1.56119	1.05047	1.13207	0.98162	1.00417	0.88162	1.00417
1.10222	0.64849	0.90715	1.20184	1.82765	1.06521	0.97426	1.08611	1.20323	1.08611
1.12308	0.88796	0.90490	1.64385	1.03635	0.82794	1.17116	0.87731	0.54002	0.61079
1.41386	1.14723	2.25714	0.97061	2.07061	1.58424	1.23885	1.07795	1.07795	1.07795
0.88535	1.06172	1.08894	1.08894	0.97426	1.07795	1.07795	1.07795	0.97426	0.97426
1.26079	1.26079	1.26079	1.26079	1.26079	1.26079	1.26079	1.26079	1.26079	1.26079
Average	1.00100	0.95066	1.08906	1.21665	1.31240	1.29706	1.08951	1.04546	0.93225
SD	0.28148	0.24571	0.36713	0.34481	0.44132	0.556494	0.30703	0.29379	0.24493
Table 3									
	N2		IDR		N2		IDR		
	2.5xIDV	1.25xIDV	2.5xIDV	1.25xIDV	2.5xIDV	1.25xIDV	2.5xIDV	1.25xIDV	
0.61294	0.73380	1.20442	1.08868	1.62036	1.48770	1.04047	1.03034	0.81930	0.71886
1.85271	0.90001	1.43402	0.96689	1.07834	0.70386	0.71886	0.88838	0.67382	0.88838
0.89128	0.89118	0.86754	1.51038	0.72955	1.42943	1.89817	1.46689	1.64226	1.46689
1.07028	0.80218	0.87711	1.07028	1.07021	0.86505	1.08842	1.62233	1.02303	1.02303
0.93039	0.93039	0.93039	1.07028	1.07021	1.23286	0.82117	1.81072	1.43836	1.43836
0.62742	1.07028	1.04885	1.51038	0.91136	1.54212	0.81930	0.97804	0.81930	0.97804
0.81372	1.03001	0.88865	1.51038	1.08882	2.80336	1.79971	0.81930	1.20399	1.20399
0.84278	1.24936	1.06432	1.96933	1.08882	0.82549	1.39914	1.00752	0.63962	0.88103
0.79891	0.81280	0.94011	1.06670	1.03643	0.94882	1.15139	1.10654	1.20075	0.93842
0.94656	1.15110	0.84207	1.05465	1.25811	0.82029	0.80535	0.93134	1.20075	0.93134
0.84656	1.11361	0.84207	0.97936	2.20123	0.90311	0.93641	0.80659	0.62737	0.93641
1.05794	1.16164	1.17874	0.91441	1.05589	0.94882	0.91675	0.75374	0.91675	0.75374
1.07893	1.11281	1.51605	1.08670	1.97611	1.57367	0.89396	1.39708	1.39708	1.39708
0.91090	1.61020	0.73645	1.56119	1.05047	1.13207	0.98162	1.00417	0.88162	1.00417
1.10222	0.64849	0.90715	1.20184	1.82765	1.06521	0.97426	1.08611	1.20323	1.08611
1.12308	0.88796	0.90490	1.64385	1.03635	0.82794	1.17116	0.87731	0.54002	0.61079
1.41386	1.14723	2.25714	0.97061	2.07061	1.58424	1.23885	1.07795	1.07795	1.07795
0.88535	1.06172	1.08894	1.08894	0.97426	1.07795	1.07795	1.07795	0.97426	0.97426
1.26079	1.26079	1.26079	1.26079	1.26079	1.26079	1.26079	1.26079	1.26079	1.26079
Average	1.00100	0.95066	1.08906	1.21665	1.31240	1.29706	1.08951	1.04546	0.93225
SD	0.28148	0.24571	0.36713	0.34481	0.44132	0.556494	0.30703	0.29379	0.24493
Table 4									
	N2		IDR		N2		IDR		
	2.5xIDV	1.25xIDV	2.5xIDV	1.25xIDV	2.5xIDV	1.25xIDV	2.5xIDV	1.25xIDV	
0.61294	0.73380	1.20442	1.08868	1.62036	1.48770	1.04047	1.03034	0.81930	0.71886
1.85271	0.90001	1.43402	0.96689	1.07834	0.70386	0.71886	0.88838	0.67382	0.88838
0.89128	0.89118	0.86754	1.51038	0.72955	1.42943	1.89817	1.46689	1.64226	1.46689
1.07028	0.80218	0.87711	1.07028	1.07021	0.86505	1.08842	1.62233	1.02303	1.02303
0.93039	0.93039	0.93039	1.07028	1.07021	1.23286	0.82117	1.81072	1.43836	1.43836
0.62742	1.07028	1.04885	1.51038	0.91136	1.54212	0.81930	0.97804	0.81930	0.97804
0.81372	1.03001	0.88865	1.51038	1.08882	2.80336	1.79971	0.81930	1.20399	1.20399
0.84278	1.24936	1.06432	1.96933	1.08882	0.82549	1.39914	1.00752	0.63962	0.88103
0.79891	0.81280	0.94011	1.06670	1.03643	0.94882	1.15139	1.10654	1.20075	0.93842
0.94656	1.15110	0.84207	1.05465	1.25811	0.82029	0.80535	0.93134	1.20075	0.93134
0.84656	1.11361	0.84207	0.97936	2.20123	0.90311	0.93641	0.80659	0.62737	0.93641
1.05794	1.16164	1.17874	0.91441	1.05589	0.94882	0.91675	0.75374	0.91675	0.75374
1.07893	1.11281	1.51605	1.08670	1.97611	1.57367	0.89396	1.39708	1.39708	1.39708
0.91090	1.61020	0.73645	1.56119	1.05047	1.13207	0.98162	1.00417	0.88162	1.00417
1.10222	0.64849	0.90715	1.20184	1.82765	1.06521	0.97426	1.08611	1.20323	1.08611
1.12308	0.88796	0.90490	1.64385	1.03635	0.82794	1.17116	0.87731	0.54002	0.61079
1.41386	1.14723	2.25714	0.97061	2.07061	1.58424	1.23885	1.07795	1.07795	1.07795
0.88535	1.06172	1.08894	1.08894	0.97426	1.07795	1.07795	1.07795	0.97426	0.97426
1.26079	1.26079	1.26079	1.26079	1.26079	1.26079	1.26079	1.26079	1.26079	1.26079
Average	1.00100	0.95066	1.08906	1.21665	1.31240	1.29706	1.08951	1.04546	0.93225
SD	0.28148	0.24571	0.36713	0.34481	0.44132	0.556494	0.30703	0.29379	0.24493

Supplementary Figure 11 – Raw data for *sod-3::GFP* expression after 16 hour IDR in N2 and *Askn-1b*

	Trial 1				Trial 2				Trial 3				Trial 4			
	wt		skn1b		wt		skn1b		wt		skn1b		wt		skn1b	
	Fed	Starved	Fed	Starved	Fed	Starved	Fed	Starved	Fed	Starved	Fed	Starved	Fed	Starved	Fed	Starved
0.96566	0.22934	0.83404	0.35818	1.05107	0.56690	0.63908	0.36680	1.04940	0.45274	0.44412	0.55146	0.76918	0.40296	0.70028	0.37484	
1.62398	0.38483	0.78191	0.45013	0.92609	0.52760	0.72539	0.41102	0.79399	0.42550	0.59726	0.44170	1.02953	0.30566	0.54102	0.30255	
0.71613	0.36543	0.74251	0.39638	0.99504	0.50729	0.81670	0.38963	0.96909	0.49946	0.58375	0.42588	0.77945	0.40338	0.52134	0.36738	
1.02235	0.28345	0.42865	0.42272	1.10518	0.45137	0.59146	0.33118	1.04446	0.37857	0.65889	0.39112	1.08430	0.43237	0.59942	0.35531	
0.81442	0.43354	0.72231	0.38761	0.88898	0.65682	0.53786	0.33090	1.08540	0.46494	0.49280	0.26692	1.32758	0.43161	0.57306	0.49240	
1.02704	0.48885	0.48963	0.50980	1.18857	0.41798	0.79019	0.40103	1.06068	0.47480	0.59817	0.12649	1.05376	0.33254	0.54746	0.39813	
1.05122	0.38680	0.88581	0.39318	0.85677	0.53681	0.87376	0.37188	1.17152	0.41607	0.52868	0.16146	0.86286	0.49208	1.19209	0.40893	
0.77488	0.66653	0.95365	0.39263	0.96514	0.42642	0.76053	0.32681	0.74584	0.39974	0.60194	0.38533	1.03938	0.22693	0.51691	0.37787	
0.89746	0.32462	0.84515	0.39935	1.15326	0.52445	0.85154	0.41520	1.37638	0.52581	0.75510	0.41688	0.85486	0.35232	0.42764	0.35466	
1.24789	0.56990	0.50168	0.29711	1.04881	0.62222	0.91362	0.44565	0.91039	0.55226	0.61845	0.34693	0.94025	0.12850	0.73408	0.36161	
0.67113	0.40503	0.51936	0.32123	1.19070	0.66327	0.43696	0.32657	0.88469	0.71216	0.59880	0.48944	1.53509	0.28371	0.71506	0.40335	
0.89291	0.60951	0.84318	0.39473	0.63038	0.64571	0.49639	0.41214	0.81692	0.62118	0.57877	0.46101	1.10912	0.58622	0.40567	0.42942	
1.20411	0.42873	0.64883	0.37723		0.54454	0.68021	0.42395	0.89827	0.51817	0.74321	0.26198	0.95017	0.70402	0.52015	0.39633	
0.99398	0.43444	0.46206	0.25759		0.40089	0.63790	0.40913	1.30929	0.51719	0.66843	0.30936	0.66039	0.48688	0.73978	0.39146	
0.89801	0.53706	0.49814	0.35979		0.46747		0.43704	0.88368	0.37391	0.57613	0.53301	0.79455	0.53845	0.73534	0.39507	
0.80344	0.36800	0.91542	0.33420		0.37997				0.61659	0.42360	0.47008	0.49028	0.40875	0.67350	0.38740	
0.89047	0.46842	0.49986			0.48393				0.32626	0.51743		1.71924	0.50651		0.22553	
1.50493	0.48173	0.79359								0.85681			0.39847		0.66899	
	0.26218	0.53849								0.63942			0.52551			
										0.74374			0.34975			
Average	1.00000	0.42781	0.67917	0.37824	1.00000	0.51904	0.69654	0.38660	1.00000	0.48643	0.61128	0.37744	1.00000	0.41483	0.63393	0.37712
StD	0.25545	0.11555	0.17800	0.05949	0.16170	0.09032	0.14712	0.04156	0.18300	0.10056	0.10731	0.12426	0.30624	0.13030	0.18450	0.05424

Supplementary Figure 12 – Raw data of *hsp-4::GFP* expression after BD in N2 and Δ *skn-1b* worms

Numbers represent fold-change in *hsp-4::GFP* expression measured by whole-worm fluorescence intensity after 16-hours dietary restriction by BD. Comparisons between all groups were made using a Two-Way ANOVA test.

	Trial 1				Trial 2				Trial 3			
	N2	N2 Ero-1	skn-1b	skn-1b Ero-1	N2	N2 Ero-1	skn-1b	skn-1b Ero-1	N2	N2 Ero-1	skn-1b	skn-1b Ero-1
0.91359	2.47692	0.95138	3.25178	1.35421	4.94986	1.06344	2.90806	1.08974	9.75113	0.72563	10.86542	
0.96902	1.23569	0.74782	4.58886	0.99413	5.51237	1.14338	3.40006	0.78094	14.00767	0.86974	11.02513	
1.01261	6.12680	0.79721	4.29975	1.03214	9.02439	0.70768	10.75309	0.78671	5.24253	0.91200	8.06028	
0.75678	5.66119	0.79011	2.84602	0.87244	3.40662	0.90190	3.78285	0.84308	3.17802	0.75429	4.43819	
0.97620	4.43518	0.76514	10.11954	1.14865	16.99891	0.89643	9.22275	0.90623	8.46792	1.21768	10.29959	
1.11114	4.46500	0.93146	2.79083	0.80645	3.35334	1.01142	9.67695	1.21273	11.72239	0.69665	8.31990	
0.86594	2.15932	0.79605	3.28286	1.08446	3.79160	0.85489	3.39224	1.10310	1.34615	0.79773	5.43013	
1.10922	3.57938	0.84505	3.87591	0.91041	3.47699	0.70126	3.54736	1.20531	8.35406	0.80868	11.49888	
0.94897	1.28007	0.72071	2.41744	1.01708	5.09884	0.76253	9.39130	0.90814	11.77887	0.94931	11.16484	
0.92872	3.72063	0.76817	6.94718	1.01070	14.39850	0.69095	3.06591	1.16311	10.08434	0.84363	4.15552	
0.94830	2.33270	0.91059	2.40262	1.44873	8.71727	0.78960	9.50618	1.01368	5.52322	0.77268	2.70758	
0.94199	2.51299	0.61028	2.12992	0.90121	12.98195	0.74537	21.77807	0.81975	2.94634	1.06405	3.53686	
1.24759	2.90005	0.78458	1.74475	1.20489	6.30718	0.62828	1.89761	0.80739	4.33471	0.56659	4.82839	
1.02161	3.72542	0.94703	4.48281	0.92452	8.72710	0.75565	3.06578	0.85599	3.41208	0.74919	9.34050	
1.30561	2.93299	0.71816	2.79265	0.86339	4.69159	0.86870	2.24737	0.80806	3.11793	0.86690	10.79584	
0.89440	1.15183	0.78222	4.19785	0.71314	6.75992	0.74274	5.83696	1.25720	5.38062	0.90241	2.58511	
1.04831	2.95077	0.93323	2.12344	0.76844		0.66227	2.49100	1.41061	4.21784	0.94404	13.13823	
	2.47113			0.94501		0.75541	4.91068	1.06346	4.89899	0.92744	8.38886	
	3.60380					0.92327	8.81488	0.96476	7.65332	0.75020		
						0.74131	3.50920		15.29823	0.92597		
							20.42440		4.76617			
									9.49382			
Average	1.00000	3.14325	0.81172	3.78201	1.00000	7.38728	0.81732	6.83918	1.00000	7.04438	0.85224	7.80996
StD	0.13531	1.37167	0.09556	2.06969	0.19317	4.18683	0.13811	5.57831	0.18788	3.86602	0.14099	3.44632

Supplementary Figure 13 – Raw data of *hsp-4::GFP* expression after *ero-1* RNAi in N2 and Δ *skn-1b* worms

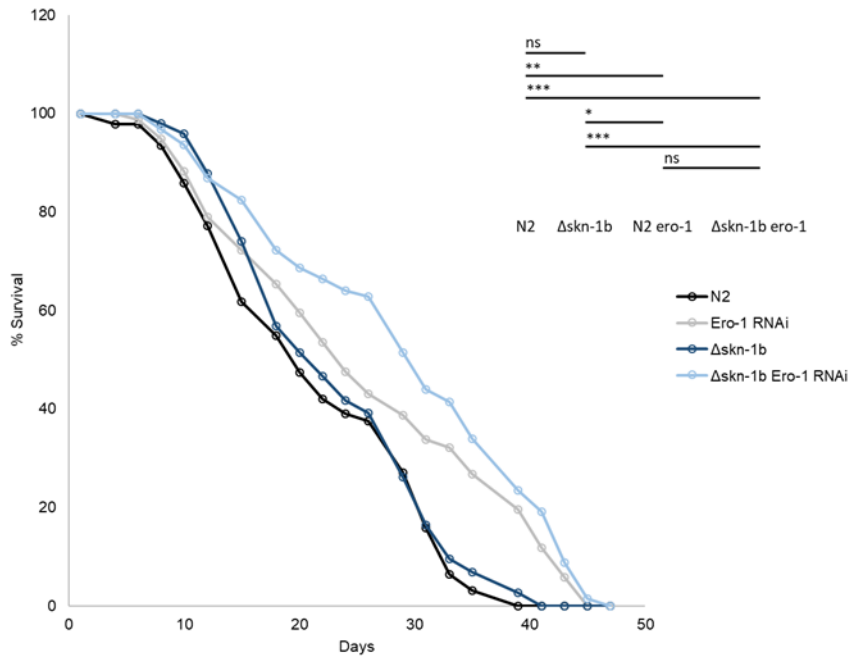
Numbers represent fold-change in *hsp-4::GFP* whole worm fluorescence intensity after 24-hours feeding on *ero-1* RNAi. Statistical significance was determined by One-Way ANOVA testing.

A

Trial 1									
N2		N2 Ero-1		Δskn-1b		Δskn-1b Ero-1			
Time (days)	Percent survival	Time (days)	Percent survival	Time (days)	Percent survival	Time (days)	Percent survival	Time (days)	Percent survival
1	100	1	100	1	100	1	100	1	100
4	97.849462	4	100	4	100	4	100	4	100
6	97.849462	6	98.717949	6	100	6	100	6	100
8	93.548387	8	94.821188	8	97.959184	8	96.808511	8	96.808511
10	85.933983	10	88.326586	10	95.918367	10	93.58156	10	93.58156
12	77.231808	12	78.958614	12	87.755102	12	86.897163	12	86.897163
15	61.785446	15	72.267206	15	74.010327	15	82.383025	15	82.383025
18	54.920397	18	65.318437	18	56.848512	18	72.226214	18	72.226214
20	47.431252	20	59.512353	20	51.485445	20	68.731397	20	68.731397
22	42.010537	22	53.561118	22	46.696101	22	66.401519	22	66.401519
24	39.009785	24	47.609883	24	41.780722	24	64.030036	24	64.030036
26	37.509408	26	43.146456	26	39.248557	26	62.798689	26	62.798689
29	27.006774	29	38.68303	29	26.165705	29	51.494925	29	51.494925
31	15.886338	31	33.847651	31	16.525708	31	43.959082	31	43.959082
33	6.354535	33	32.155268	33	9.639996	33	41.447135	33	41.447135
35	3.177268	35	26.796057	35	6.885712	35	33.911292	35	33.911292
39	0	39	19.650442	39	2.754285	39	23.477048	39	23.477048
41	0	41	11.790265	41	0	41	19.075102	41	19.075102
43	0	43	5.895133	43	0	43	8.803893	43	8.803893
45	0	45	0	45	0	45	1.467316	45	1.467316
47	0	47	0	47	0	47	0	47	0

Restricted mean				Age in days at % mortality					
Name	N	Days	S.E.	95% C. I.	25%	50%	75%	90%	100%
N2	100	21.58	0.98	19.65 ~ 23.51	15.00	20.00	31.00	33.00	39.00
N2 ero-1(-)	80	25.90	1.41	23.13 ~ 28.67	15.00	24.00	39.00	43.00	45.00
skn-1b(-)	100	23.22	0.89	21.47 ~ 24.97	15.00	22.00	31.00	33.00	41.00
skn-1b(-) ero-1(-)	100	29.35	1.24	28.92 ~ 31.78	18.00	31.00	39.00	43.00	47.00

Statistics			
condition	chi	pvalue	corrected_pvalue
N2 v.s. N2 ero-1(-)	9.47	0.0021	0.0063
N2 v.s. skn-1b(-)	1.1	0.2944	0.8833
N2 v.s. skn-1b(-) ero-1(-)	26.17	3.10E-07	9.40E-07
N2 ero-1(-) v.s. N2	9.47	0.0021	0.0063
N2 ero-1(-) v.s. skn-1b(-)	6	0.0143	0.043
N2 ero-1(-) v.s. skn-1b(-) ero-1(-)	2.69	0.1011	0.3033
skn-1b(-) v.s. N2	1.1	0.2944	0.8833
skn-1b(-) v.s. N2 ero-1(-)	6	0.0143	0.043
skn-1b(-) v.s. skn-1b(-) ero-1(-)	21.34	0.000038	0.00012
skn-1b(-) ero-1(-) v.s. N2	26.17	3.10E-07	9.40E-07
skn-1b(-) ero-1(-) v.s. N2 ero-1(-)	2.69	0.1011	0.3033
skn-1b(-) ero-1(-) v.s. skn-1b(-)	21.34	0.000038	0.00012

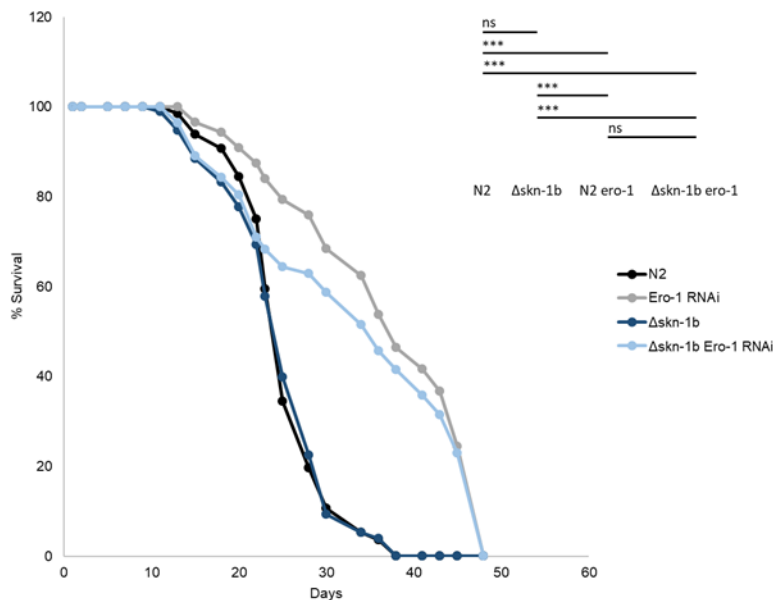


B

Trial 1									
N2		N2 Ero-1		Δskn-1b		Δskn-1b Ero-1			
Time (days)	Percent survival	Time (days)	Percent survival	Time (days)	Percent survival	Time (days)	Percent survival	Time (days)	Percent survival
1	100	1	100	1	100	1	100	1	100
2	100	2	100	2	100	2	100	2	100
5	100	5	100	5	100	5	100	5	100
7	100	7	100	7	100	7	100	7	100
9	100	9	100	9	100	9	100	9	100
11	100	11	100	11	98.958333	11	100	11	100
13	98.484848	13	100	13	94.791667	13	96.428571	13	96.428571
15	93.795094	15	96.690909	15	88.472222	15	89.104882	15	89.104882
18	90.668591	18	94.318182	18	83.206019	18	84.222423	18	84.222423
20	84.415684	20	90.909091	20	77.658961	20	80.394131	20	80.394131
22	75.036075	22	87.5	22	69.296679	22	71.014816	22	71.014816
23	59.403559	23	84	23	57.746399	23	68.335012	23	68.335012
25	34.391534	25	79.333333	25	39.780853	25	64.315305	25	64.315305
28	19.652305	28	75.833333	28	22.542483	28	62.917146	28	62.917146
30	10.719438	30	68.49424	30	9.282199	30	58.627341	30	58.627341
34	5.35972	34	62.379032	34	5.304114	34	51.477665	34	51.477665
36	3.573146	36	53.817204	36	3.978085	36	45.757924	36	45.757924
38	0	38	46.478496	38	0	38	41.468119	38	41.468119
41	0	41	41.586022	41	0	41	35.748378	41	35.748378
43	0	43	36.693548	43	0	43	31.458573	43	31.458573
45	0	45	24.462366	45	0	45	22.878962	45	22.878962
48	0	48	0	48	0	48	0	48	0

Name	N	Restricted mean			Age in days at % mortality				
		Days	S.E	95% C.I	25%	50%	75%	90%	100%
N2	80	25.26	0.66	23.96 ~ 26.55	23	25	28	34	38
Ero-1 (-)	100	36.81	1.1	34.66 ~ 38.96	30	38	45	48	48
skn-1b	100	24.8	0.64	23.54 ~ 26.05	22	25	28	30	38
skn-1b Ero-1 (-)	100	33.72	1.37	31.03 ~ 36.42	22	36	45	48	48

condition	dhi	Statistics		
		pvalue	corrected_pvalue	
N2 v.s. Ero-1 (-)	62.99	0	0	
N2 v.s. skn-1b	0	0.9714	1	
N2 v.s. skn-1b Ero-1 (-)	28.9	7.60E-08	2.30E-07	
Ero-1 (-) v.s. N2	62.99	0	0	
Ero-1 (-) v.s. skn-1b	71.05	0	0	
Ero-1 (-) v.s. skn-1b Ero-1 (-)	1.14	0.2857	0.857	
skn-1b v.s. N2	0	0.9714	1	
skn-1b v.s. Ero-1 (-)	71.05	0	0	
skn-1b v.s. skn-1b Ero-1 (-)	34.9	3.50E-09	1.10E-08	P>0.05 ns
skn-1b Ero-1 (-) v.s. N2	28.9	7.60E-08	2.30E-07	P<0.05 *
skn-1b Ero-1 (-) v.s. Ero-1 (-)	1.14	0.2857	0.857	P<0.001 **
skn-1b Ero-1 (-) v.s. skn-1b	34.9	3.50E-09	1.10E-08	P<0.0001 ***



Supplementary Figure 15– Raw *ero-1* RNAi lifespan data

Two independent lifespan trials (A; trial 1, B; trial 2) of *ero-1* RNAi in N2 and Δ *skn-1b* worms were carried out. Both independent trials showed similar effects of a significant extension of lifespan in *ero-1* RNAi conditions that did not require SKN-1B.

	Trial 1				Trial 2				Trial 3			
	N2 Fed	N2 Starved	skn1b Fed	skn1b Starved	N2 Fed	N2 Starved	skn1b Fed	skn1b Starved	N2 Fed	N2 Starved	skn1b Fed	skn1b Starved
	1.204114454	0.788700482	0.98988833	0.555163881	0.95123445	0.801458897	0.830827944	0.708281316	0.876116199	0.848920198	0.707277105	0.56968378
	0.825773965	0.711689047	1.011388316	0.901830577	1.03415101	0.616832294	0.697481935	0.636274471	0.796240294	0.691275584	0.878272783	0.941719142
	0.903904849	0.773406848	0.816176345	0.691967008	0.983863066	0.698749546	0.76502745	0.653839927	0.88775166	0.81614342	0.809015171	0.755841392
	1.107166967	1.072266531	0.804125817	0.531243912	1.230191007	0.851060319	0.617523718	0.811830253	1.01334735	0.88365601	0.699720831	0.735641941
	1.106952955	0.899081345	0.977173903	0.765603637	1.044691893	0.747198595	0.963367291	0.652704017	1.124172699	0.607020662	0.790198567	0.640521789
	1.102096527	0.80941027	1.034468699	0.58901072	1.076579698	0.767677908	0.629294384	0.796915255	1.133367179	0.742292779	0.86605763	0.680344504
	1.02734045	0.66725684	0.965886049	0.752795835	0.901270853	0.558604537	0.815517946	0.827551912	0.91929627	0.927001694	0.934821367	0.661511438
	0.970512008	0.257226096	1.060545252	0.648176837	1.011684641	0.681579189	0.883507948	0.460060191	1.031918333	0.7446963	0.86605763	0.43370376
	0.961572881	0.867144153	0.793491061	0.723245701	0.868708087	0.599365613	0.888150265	0.630150432	1.001558904	0.684970458	0.909222226	0.414014662
	0.977146378	0.70999413	0.871375008	0.696082625	0.7998785	0.47138637	0.815715396	0.815715396	0.943358804	0.852097455	0.775793906	0.603330069
	1.060858039	0.699704369	0.945291498	0.765850574	0.90171534	0.630315057	1.049284922	0.70877519	1.003540327	0.684970458	0.806298863	0.634529449
	1.011157842	0.631878992	0.924812186	0.88765639	0.981920495	0.70032943	0.760845983	0.513382132	1.254794827	0.716808875	0.875342463	0.634529449
	0.97082479	0.788321846	1.03940744	0.832424803	0.924861573	0.979730986	0.938492498	0.716808875	1.065585731	0.716808875	0.952913622	0.717911861
	0.953703821	0.545582723	1.044691893	0.697399623	0.899245969	0.779563811	0.983632591	0.652111368	1.054083403	0.652111368	0.934821367	
	0.950427789	0.608930308	0.809393807	0.832572965	0.899245969	0.735674866	0.731493399	0.652111368	1.001558904	0.970259139	0.934821367	
	0.843108946	0.830729169	0.913289457	0.872181669	1.087477853	0.678204383	0.797458517	0.746177922	0.943358804	0.746177922	0.943358804	
	1.029480571	0.83007067	0.974380683	0.76053196								
	1.206945999	0.853941252	0.933356208	0.872181669			1.056479022					
	1.023735169	0.913946955	1.081419664	0.60282732			0.542553629					
	0.927199244	0.785440913	0.786889611	0.575890131			0.777143828					
	1.1239093	0.756911453	0.748795455	0.821641885								
		1.040164714	0.848706196	0.74336284								
			0.846039266	0.615663459								
			0.862962685	0.553715183								
			0.846450828	0.650827295								
			0.791630802	0.54380476								
			0.855422874	0.757718114								
			0.868905637	0.610066219								
			0.79701403	0.567016859								
Average	1.013711092	0.76553629	0.904944255	0.698349337	0.93060967	0.717767572	0.826844026	0.686800879	1.001312449	0.779807456	0.84259861	0.649063067
S.D	0.108216932	0.17023197	0.097107938	0.111290806	0.103035337	0.126768794	0.141594362	0.103625505	0.10907373	0.101708053	0.085477679	0.141653418

Appendix 16 – Raw data of mitochondrial % coverage in body wall muscle of N2 and Δ skn-1b worms

Numbers represent the fold change in area coverage of mitochondria as a percentage of whole muscle fibres in N2 or Δ skn-1b worms; in fed conditions or after 16 hours starvation by BD. Below, statistical significance was determined by comparison of groups with a One-Way ANOVA test.